

CREEP ALONG A DISCONTINUITY IN GRANITE

By



AHMED MOHAMED GADI

A Thesis

Presented to the University of Manitoba
in Partial Fulfillment of the
Requirements for the Degree of
Master of Science in Civil Engineering

Winnipeg, Manitoba

APRIL, 1986

Permission has been granted to the National Library of Canada to microfilm this thesis and to lend or sell copies of the film.

The author (copyright owner) has reserved other publication rights, and neither the thesis nor extensive extracts from it may be printed or otherwise reproduced without his/her written permission.

L'autorisation a été accordée à la Bibliothèque nationale du Canada de microfilmer cette thèse et de prêter ou de vendre des exemplaires du film.

L'auteur (titulaire du droit d'auteur) se réserve les autres droits de publication; ni la thèse ni de longs extraits de celle-ci ne doivent être imprimés ou autrement reproduits sans son autorisation écrite.

ISBN 0-315-34062-2

CREEP ALONG A DISCONTINUITY IN GRANITE

BY

AHMED MOHAMED GADI

A thesis submitted to the Faculty of Graduate Studies of
the University of Manitoba in partial fulfillment of the requirements
of the degree of

MASTER OF SCIENCE

© 1986

Permission has been granted to the LIBRARY OF THE UNIVERSITY OF MANITOBA to lend or sell copies of this thesis, to the NATIONAL LIBRARY OF CANADA to microfilm this thesis and to lend or sell copies of the film, and UNIVERSITY MICROFILMS to publish an abstract of this thesis.

The author reserves other publication rights, and neither the thesis nor extensive extracts from it may be printed or otherwise reproduced without the author's written permission.

To: My wife Fatma
My daughter Rouida
My parents

ACKNOWLEDGEMENTS

I am deeply indebted to many people for their part in making this work possible. In particular, my sincere gratitude goes to Dr. Emery Zoltan Lajtai for initiating this investigation, for his guidance and invaluable advice throughout the whole project and during the preparation of this thesis. A special thank you is also extended to Mr. Wojciech Grajewski for his assistance and advice.

I would also like to extend my thanks to Drs. A. Soliman and B. Stimpson for reviewing this thesis work.

The assistance of the technical staff, especially Mr. Ed Lemke and Mr. John Clark, is much appreciated.

I also wish to thank Mrs. Ingrid Trestrail for doing an excellent job with the typing of this thesis and for her patience.

A special thank you is also extended to the Civil Engineering Department, El Fateh University in Libya for supporting me in undertaking the Master's programme at the University of Manitoba.

Finally, a very special and deep thank you goes to my wife Fatma, my daughter Rouida, my parents, my brothers and sisters, for their encouragement and understanding in allowing me to devote so many long days away from home over the period of my study.

Thank you, my advisor, Dr. Emery Lajtai

Thank you, my wife, Fatma

ABSTRACT

The mechanism of frictional sliding on a flat and worn discontinuity in granite has been examined. Over 100 direct shear tests were conducted using a normal stress between 2 and 14 MPa acting on an initially artificial, saw-cut surface in Lac du Bonnet granite. The final test surface was prepared by repeated but always one-directional shearing of the discontinuity.

Frictional sliding under increasing shear load progresses in a "stick-slip" manner. During "stick-slip" events, the shear load cycles between high and low limits and the shear load versus shear displacement curve displays corresponding "steps" (rise in load) and "risers" (fall in load). At high normal load, these features tend to be "rounded-off" to create the appearance of a full, transient to tertiary, creep curve. During stick-slip events, the trend of normal displacement is downward, signifying progressive closure at the discontinuity.

In order to have increasing shear displacement, the shear load (or its trend when stick-slip occurs) must continuously increase otherwise displacement comes to a halt within a few hours. At constant shear load (creep conditions) there is only transient creep. The shear load must again be increased to start movement again. There seems to be no end to this process, and therefore long-term strength should increase with time and displacement, perhaps indefinitely. In this research program, this was limited by the total displacement allowed by the shear box that is about 25 mm. This would typically produce an increase in shear strength corresponding to a friction

angle of 27° at first slip to 32° at the end of a 15 day long test.

The experimental results can be interpreted in terms of the widely accepted "adhesion theory of friction". Accordingly, frictional resistance is determined by the true area of contact at junctions and the strength of these junctions. Assuming that this strength is constant in our experiments, the increase in frictional resistance with time and movement would come from an increase in the area of true contact at joining asperities. In particular, increase in strength without "stick-slip" type of shear displacement could be caused by increasing the true area of contact through the creep of the asperities. Increasing strength with substantial shear displacement, as it usually occurs in a "stick-slip" manner, would be the result of fracture at asperities. In this case, the increase in contact area would come from two sources: from the smearing of gouge at the fractured sites and from the development of new contacts as asperities of lesser heights come in contact through closure between the rock blocks on either side of the discontinuity.

TABLE OF CONTENTS

| | <u>Page</u> |
|---|-------------|
| ACKNOWLEDGEMENT | (i) |
| ABSTRACT | (ii) |
| TABLE OF CONTENTS | (iv) |
| LIST OF TABLES | (vi) |
| LIST OF FIGURES | (vii) |
| INTRODUCTION | 1 |
| CHAPTER 1 THE THEORY OF FRICTION | 3 |
| 1.1 Friction in the Earlier Scientific Literature | 3 |
| 1.2 Amonton's Law of Friction | 4 |
| 1.3 Coulomb's Roughness Theory | 5 |
| 1.4 Adhesion Theory of Friction in the Earlier Scientific Literature | 8 |
| 1.5 The Modern Adhesion Theory of Friction | 9 |
| 1.6 Amonton's Law by the Adhesion Theory | 11 |
| CHAPTER 2 FRICTION AND THE TIME-DEPENDENCE BETWEEN ROCK SURFACES | 14 |
| 2.1 Friction Between Rock Surfaces | 14 |
| 2.2 The Time-Dependence of Friction on Rock Surfaces | 15 |
| 2.2.1 Mechanism of Time-Dependency | 20 |
| 2.3 Stick-Slip Phenomena | 21 |
| CHAPTER 3 TEST SPECIMEN | 24 |
| 3.1 Test Specimen | 24 |
| 3.1.1 Rock Type | 24 |
| 3.1.2 Selection and Preparation of Test Specimen | 25 |
| 3.2 Testing Equipments and Set Up | 28 |
| 3.2.1 Direct Shear Machine | 28 |
| 3.2.2 Normal and Shear Loading RAMs | 28 |
| 3.2.3 Transducers | 28 |
| 3.3 Calibration of Pressure and LVDT Transducers | 28 |
| 3.4 Final Set Up | 30 |
| 3.5 Shear Load Correction for Travel | 30 |
| CHAPTER 4 LABORATORY INVESTIGATION | 35 |

| | <u>Page</u> |
|--|-------------|
| 4.1 Basic Friction Angle ϕ_b | 35 |
| 4.1.1 Direct Shear Test | 35 |
| 4.1.2 Tilt Table Test | 36 |
| 4.2 The Influence of Loading Rate on the Frictional Resistance | 36 |
| CHAPTER 5 LABORATORY INVESTIGATION OF THE TIME-DEPENDENCY OF FRICTION | 40 |
| 5.1 Effect of Normal Load History on the Static Coefficient of Friction | 40 |
| 5.2 Long-Term Strength Along the Discontinuity . | 42 |
| 5.3 Description of the Shape of Load and Displacement Curves | 44 |
| CHAPTER 6 DISCUSSIONS, SUMMARY AND CONCLUSION | 59 |
| 6.1 Summary of Results | 59 |
| 6.2 Interpretation of Results in Terms of the Adhesion Theory | 62 |
| REFERENCES | 70 |

LIST OF TABLES

| <u>Table</u> | | <u>Page</u> |
|--------------|---|-------------|
| 2.1 | Coefficient of friction of rocks and minerals (Jaeger and Cook, page 59) | 16 |
| 4.1 | The influence of loading rate on the frictional resistance | 39 |
| 5.1 | Influence of sticking time | 41 |
| 5.2 | Summary of experimental results of the friction on worn granite surfaces | 45 |
| 5.3a,b,c | Detailed results of friction | 46-48 |

LIST OF FIGURES

| <u>Figure</u> | | <u>Page</u> |
|---------------|---|-------------|
| 1.1a | The friction test | 6 |
| 1.1b | The friction test data interpretation | 6 |
| 1.2 | Coulomb's ideas on the interlocking of surface roughnesses (1781) | 6 |
| 1.3 | The role of surface roughness (lifting over asperities) | 13 |
| 1.4 | Adhesion of lead by Desaguliers (1683-1744) ... | 13 |
| 1.5 | Mechanism of welding and shearing | 13 |
| 2.1 | Different devices used to determine the frictional properties of rock surfaces | 18 |
| 2.2 | Typical relationship between static friction and time of stick (Rabinowicz, 1965) | 18 |
| 2.3 | Influence of sliding speed on coefficient of friction for steel, copper, chromium and nickel sliding on sapphire (Miller, 1962) | 19 |
| 2.4 | Summary of experimental results on time-dependence (Dieterich, 1972) | 19 |
| 3.1 | Location map | 25 |
| 3.2a | Sample arrangement | 27 |
| 3.2b | Direct shear machine | 29 |
| 3.3 | Air hydraulic booster system | 31 |
| 3.4 | Normal load calibration | 32 |
| 3.5 | Shear load calibration | 32 |
| 3.6 | Horizontal displacement calibration | 33 |
| 3.7 | Vertical displacement calibration | 33 |
| 3.8 | Illustration of the shear load correction | 34 |

| <u>Figure</u> | | <u>Page</u> |
|---------------|--|-------------|
| 3.9 | Shear load correction | 34 |
| 4.1 | Typical load displacement curve | 37 |
| 4.2 | Friction angle | 37 |
| 5.1 | Influence of sticking time | 43 |
| 5.2 | Influence of sticking time | 43 |
| 5.3a,b,c | The variation of the displacement with time ... | 49,50 |
| 5.4 | Normal loading application | 51 |
| 5.5 | Vertical displacement versus time | 51 |
| 5.6 | Horizontal displacement versus time | 52 |
| 5.7 | Shear load versus time | 52 |
| 5.8 | Stable sliding | 54 |
| 5.9 | Stick-slip events | 54 |
| 5.10 | Shear displacement versus time at low normal load | 55 |
| 5.11 | Shear displacement versus time at high normal load | 55 |
| 5.12 | Transient to tertiary creep curve | 56 |
| 5.13 | Vertical displacement versus time at high normal load | 58 |
| 5.14 | Vertical displacement versus time at low normal load | 58 |
| 6.1 | Displacement during stick slip | 60 |
| 6.2a | Load displacement curve | 61 |
| 6.2b | Stick slip events | 61 |
| 6.3 | Shear load versus time | 63 |
| 6.4 | Vertical displacement versus time | 63 |

| <u>Figure</u> | | <u>Page</u> |
|---------------|---|-------------|
| 6.5a,b,c,d | Shear displacement versus time | 64,65 |
| 6.6 | The end of stick-slip | 66 |
| 6.7 | The end of stick-slip | 66 |
| 6.8 | The load history of test 217 | 67 |
| 6.9 | The increase in frictional resistance with time | 67 |

INTRODUCTION

A natural rock mass consists of interlocking angular particles or blocks of hard material, intact rock, separated by discontinuity surfaces or planes of weakness, such as bedding planes, joints, faults, etc. which may or may not be coated with weaker materials. The course of a failure surface across such a mass of discontinuous rock depends chiefly on the geometry of the planes of weakness. In a simple situation, a single plane of weakness itself may lead to failure. In a more complex rock structure, however, a developing failure surface shifts from one set of discontinuities to another, cutting across solid rock bridges in the process. Therefore, the shear strength of the rock mass may be considered to consist of a combination of solid or intact rock strength in rock bridges and discontinuity strength.

When there are no macroscopic rock bridges to shear, each discontinuity, or joint of the rock mass derives its shear strength from two sources: (1) the frictional resistance offered by the two macroscopically smooth surfaces sliding relative to one another, and (2) resistance to sliding imposed by the geometry of microscopic irregularities or asperities existing on the rock surface of sliding. Intact rock strength may still be involved at this microscopic scale where asperities must often be sheared.

In addition to being dependent on surface texture, frictional resistance is also time-dependent (Dieterich, 1972, 1978; Amadei and Curran, 1980). The chief purpose of this research is to identify the mechanism that controls the sliding process on flat and smooth

rock surfaces, and in particular the dependence of frictional resistance on time. The flat and smooth surface here is defined as a "residual surface", a surface that results from repeated one-directional shearing.

CHAPTER 1

THE THEORY OF FRICTION

1.1 FRICTION IN THE EARLIER SCIENTIFIC LITERATURE

"Ever since man tried to drag loads over the ground he has been aware of the existence of friction. He may not have known how to explain it but he knew how to deal with it" (Bowden and Tabor, 1973).

The first known written remarks on friction were made by Leonardo da Vinci. In the middle of the fifteenth century Leonardo da Vinci wrote his notebooks in which he concluded, based on known facts at that time, that "Friction produces double the amount of effort if the weight be doubled". He also added that the friction is independent of the apparent contact area. He had not mentioned "force" simply because his notebooks had been written two hundred years before Newton had given a clear definition of force.

Bowden and Tabor (1973) reported that the first "scientific" studies of friction were carried out in France for military needs. However, the first original work on friction was due to Guillaume Amonton (1663-1705). In 1699 he published a paper in the Proceedings of the French Royal Academy of Science on friction. In this work he rediscovered the two forgotten laws of friction originally derived by Leonardo da Vinci (1452-1519). The French Royal Academy instructed their senior academician, De La Hire (1640-1718) to repeat Amonton's experiments and check their validity. This he did and confirmed Amonton's conclusions. Amonton's law of friction has remained with us to this day as a very good working approximation.

1.2 AMONTON'S LAW OF FRICTION

At first approximation, friction is defined through Amonton's law stating that the maximum amount of frictional resistance (F) in a plane of sliding is directly proportional to the normal load (N) on the plane through a constant of proportionality known as the coefficient of friction (μ).

$$F = \mu N \quad (1.1)$$

The coefficient of friction is a property of the material, usually determined by friction tests (Fig. 1.1a). The maximum amount of friction available (F) at a constant normal load (N) is equal in magnitude to the load (T), applied tangentially to the plane of frictional movement, that is necessary to initiate sliding.

The coefficient of friction may be found from a single test, although it is more common to determine the load (T) at several values of normal load (N) and then plot the results in a $F - N$ diagram (Fig. 1.1b). The straight line fitted to the experimental points has a slope which should give the coefficient of friction (μ).

$$\mu = \tan \phi \quad (1.2)$$

where ϕ is called the angle of friction.

It is common practice to express the normal and shear loads in terms of corresponding stress components. This may be found by dividing equation (1.1) by the area of apparent contact A :

$$\tau = \frac{F}{A} \text{ and } \sigma = \frac{N}{A} \quad (1.3)$$

Therefore Amonton's law becomes:

$$\tau = \mu \sigma = \sigma \tan \phi \quad (1.4)$$

Amonton's law of friction may therefore be summarized in

two statements:

1. The friction force is proportional to the normal load with the constant of proportionality being the coefficient of friction.
2. The friction force is independent of the size of the apparent contact area.

1.3 COULOMB'S ROUGHNESS THEORY

Charles Augustin Coulomb, a Captain in the French Royal Corps of Engineers (1736-1806), began his research on friction in 1779. He recognized that most of the surfaces he worked with were not smooth. When two such surfaces are placed together, the contact resembles the interlocking bristles of two brushes placed against one another (Fig. 1.2). Coulomb felt friction could arise from surface roughness, due to the work done in dragging one surface up the roughnesses of the other, lifting it over the asperities. This can be illustrated as shown in (Fig. 1.3). If the top surface pushed by force F moves from point A to point C , then the work done is $F \times \overline{AB}$. Where the work done on the load W in overcoming gravity is $W \times \overline{CB}$, therefore:

$$F \times \overline{AB} = W \times \overline{CB} \quad (1.5)$$

$$F = W \frac{\overline{CB}}{\overline{AB}} = W \tan \theta \quad (1.6)$$

$$\text{and } \frac{F}{W} = \tan \theta \quad (1.7)$$

Hence $\frac{F}{W} = \mu$

which is Amonton's law

$$\text{then } \mu = \tan \theta \quad (1.8)$$

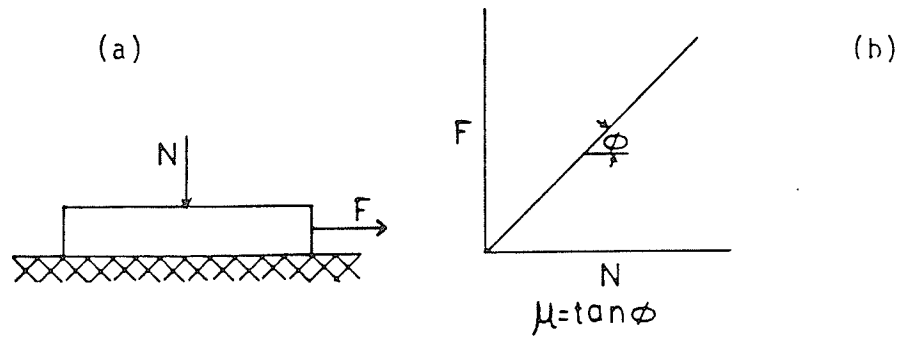


Fig. 1.1 The friction test: a) the test b) data interpretation

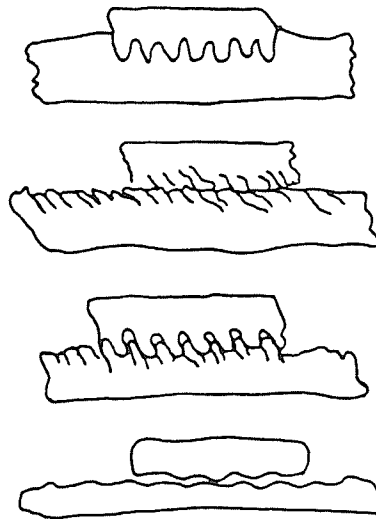


Fig. 1.2 Part of an illustration from Coulomb's book: Theory of Simple Machines (page I.II), Published in 1781, which shows his ideas on the interlocking of surface roughnesses

From this, the coefficient of friction does not depend on the load but is determined only by the slope of the roughness ($\tan \theta$). In addition, the size of the surface is out of consideration.

Now let us consider what will happen a little later when the contact regions have moved to the other side of the slope. Clearly the body slides downslope and hence exerts a horizontal force in the direction of sliding. Bowden and Tabor (1973) wrote that "A little thought shows that the work that we have to use in sliding up the slopes is restored to us in sliding down the slopes. If friction is due only to the overcoming of gravity, we can only do a net amount of work if we raise one body by a definite distance. But if the average position of the top body is in a horizontal straight line there is not net vertical movement. Parts of the body may be sliding up roughnesses but other parts will be sliding down equivalent slopes somewhere else or at a later instant. The frictional force would therefore fluctuate between positive and negative and its average value would be zero. Consequently no energy could be lost in moving one body over another in a horizontal plane. This criticism of the roughness theory was put forward in 1804 by John Leslie (1766-1832), Professor of Physics in the University of Edinburgh, and remains unanswered."

Interestingly, the concept of "dragging the rock up and over asperities" was revived some two hundred years later by Newland and Alleyly (1957) and in particular by Patton (1966) in rock mechanics. However, the challenge to the roughness theory by Leslie has been more or less forgotten.

1.4 ADHESION THEORY OF FRICTION IN THE EARLIER SCIENTIFIC LITERATURE

During approximately the same period when Amonton published his paper on friction, scientists in England were discovering cohesion. Jean Theophile Desaguliers (1683-1744), an English physicist, discovered cohesion between clean, like solids. He described his work on the adhesion of lead (Fig. 1.4).

"I took the leaden balls and having from each of them cut off a segment of about $\frac{1}{4}$ inch in diameter, I pressed them together with my hand, with a little twist, to bring the flat parts to touch as well as I could. The balls stuck so fast, that the lower one was sustained though loaded with the scales and the weights E which amounted to 16 pounds. A little more weight added separated them and, upon viewing the touching surfaces, it appeared that they did not exceed a circle of $\frac{1}{10}$ inch diameter" (Bowden and Tabor, 1973). Although Desaguliers provided a different approach to friction, by introducing adhesion, his ideas were not fully developed. He recognized adhesion played a part in friction but he could not see how to explain the two laws of friction, since adhesion does depend on the area of contact. A similar confusion evidently existed in the mind of Coulomb, for he considered the possibility of adhesion but rejected it because adhesion would imply that the friction would double if one doubled the number of contact regions, that is, if one doubled the area of contact (Bowden and Tabor, 1973).

This apparent contradiction has been resolved by the modern adhesion theory of friction.

1.5 THE MODERN ADHESION THEORY OF FRICTION

A great deal of study has been devoted to the frictional properties of metals. It has been shown on a microscopic scale that even the best-prepared surfaces are rough and contain asperities. When such two surfaces are placed in contact they will touch at the tips of mating asperities. A theory to explain the frictional resistance between such metal surfaces has been proposed by Bowden, Moore and Tabor (1943). Their theory stated that the adhesive forces at the points of contact are so strong that cold welding actually takes place and therefore, the frictional resistance that can be developed is equal to the product of the real contact area and the shear strength of the metal junction. Terzaghi (1925) proposed that the frictional force developed between two clean, dry, mineral surfaces was the result of molecular bonds (adhesion) formed at the contacts between the surfaces. He theorized that the friction which could be developed was equal to the product of the true contact area and the unit shear strength of the bonds. Terzaghi (1925) suggested that the true area of contact should be related to the normal load and the yield stress of the material. Bowden and Tabor (1954) measured the true contact area of metals by electrical and optical means and concluded that the true area of contact can be derived from Hertz's equations describing the contact between a sphere and a flat surface by assuming elastic conditions at the contact. The region of contact is a circle of diameter:

$$d = 1.75 (N \times r (\frac{1}{E_1} + \frac{1}{E_2}))^{1/3} \quad (1.9)$$

where E_1 and E_2 are Young's moduli for the two surfaces and N is the load and r is the radius of the sphere.

Since the true area of contact $A_t = \frac{\pi d^2}{4}$
 then $d = \left(\frac{4A_t}{\pi}\right)^{\frac{1}{2}}$ or

$$d = 1.27 A_t^{\frac{1}{2}} \quad (1.10)$$

From equations (1.9) and (1.10)

$$A_t = 2.4 (N \times r \left(\frac{1}{E_1} + \frac{1}{E_2}\right))^{\frac{2}{3}} \quad (1.11)$$

Since r , E_1 , E_2 are constants

$$\text{then } A_t = K N^{\frac{2}{3}} \quad (1.12)$$

where K is constant.

Accordingly the area of contact is a function of the load alone. In particular it is proportional to $N^{\frac{2}{3}}$.

Since the mean pressure P_m over the circle of contact has the value

$$P_m = \frac{N}{A_t} \quad \text{or} \quad A_t = \frac{N}{P_m} \quad (1.13)$$

From equations (1.12) and (1.13)

$$P_m = K N^{\frac{1}{3}} \quad (1.14)$$

Moore (1975) however suggested that equation (1.12) does not apply when the asperities are of variable heights. Practical surfaces exhibit a normal distribution of asperity height in which case the actual contact area is directly proportional to the load:

$$A_t = K N \quad (1.15)$$

The same conclusion is reached if plastic deformation is assumed at the contact. As the load increases the mean pressure increases as well according to equation (1.14) until it reaches a value at which the elastic limit of one of the metals is exceeded. At this stage, plastic deformation begins. As the load is further increased the plastic region grows, until the whole area of contact

deforms plastically where the mean pressure becomes the yield stress, P . With a further increase in load, the mean pressure remains constant, but the true area of contact increases through plastic deformation (Bowden and Tabor, 1954):

$$N = AP \text{ or } A = \frac{1}{P} N \quad (1.16)$$

1.6 AMONTON'S LAW BY THE ADHESION THEORY

It is possible to interpret Amonton's law in terms of the adhesion theory. As previously stated, if two surfaces contact only at the tip of the asperities, the true area for a single given asperity (Fig. 1.5) is found to be proportional to the normal load:

$$A_1 = \frac{N_1}{P} \quad (1.17)$$

where P is defined as the yield stress, load N_1 divided by the surface area of the contact A_1 .

For this asperity to slide relative to its mate, the junction must be sheared. If S is the mean tangential stress required to shear the junction, the tangential force required to shear a single contact:

$$F_1 = A_1 S \quad (1.18)$$

Combining equation (1.17) and (1.18):

$$F_1 = \frac{N_1}{P} S \quad (1.19)$$

For the whole area of contact, where there are n contacts the total force to shear all n contacts:

$$F = n F_1$$

and the total normal force:

$$N = n N_1$$

$$\text{From this } F = N \frac{S}{P} \quad (1.20)$$

Therefore F becomes directly proportional to the normal load.

$$\text{Since } A = \frac{N}{P} \text{ and } A = \frac{F}{S} \text{ then}$$

$$\frac{N}{P} = \frac{F}{S} \text{ i.e. } \frac{F}{N} = \frac{S}{P} = \mu \quad (1.21)$$

Thus $\mu = \frac{S}{P}$. This is Amonton's first law. This shows that μ is related to the two constants of the materials in contact. Both these properties depend on the plastic properties of the material and do not depend upon the size of the body. This is Amonton's second law.

Bowden and Tabor (1954) emphasized that adhesion at points of contact will be greatly influenced by the presence of surface films. In the previous case we assumed that the surfaces were clean, in the chemical sense, whereas most surfaces have some form of contamination. Thus many metals are covered with oxide films in air, whilst on many surfaces thin lubricant films are present. This contamination develops shear strength S_1 over a real contact area of $A(1-\rho)$, if ρ is the fraction of non-contaminated contact area. The friction force will be:

$$F = A (\rho S + (1-\rho) S_1). \quad (1.22)$$

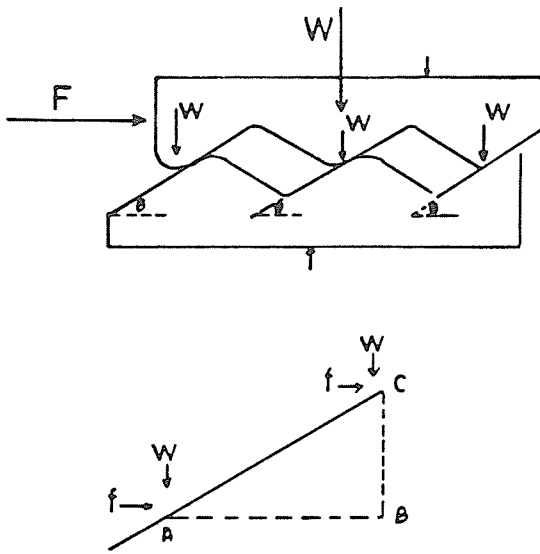


Fig. 1.3 A body of weight W rests on a surface making an angle θ to the surface. The horizontal force f necessary to push the body up the slope against gravity moves a horizontal distance AB , while the load W moves a vertical distance BC (Bowden and Tabor, 1973, page 21)

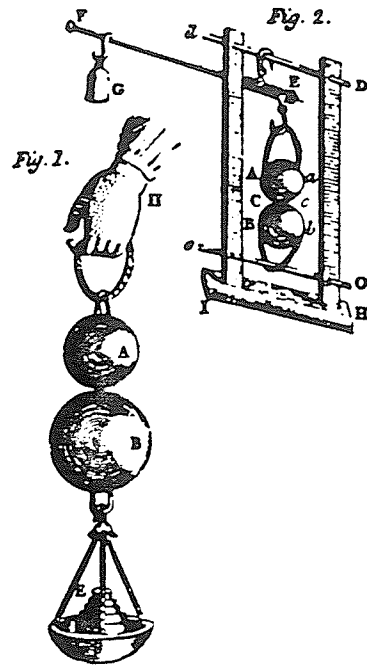


Fig. 1.4 Figures from a paper published by Desaguliers (1683-1744) on the adhesion of lead (Bowden and Tabor, 1973, page 15)

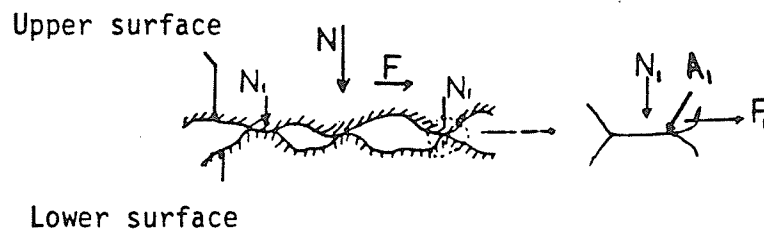


Fig. 1.5 Mechanism of welding and shearing

CHAPTER 2

FRICTION AND TIME-DEPENDENCE BETWEEN ROCK SURFACES

2.1 FRICTION BETWEEN ROCK SURFACES

Much less work has been done on the friction of minerals and rocks than on metals. Nevertheless, the reported phenomena on metals and the observed phenomena on rocks are much the same (Jaeger and Cook, 1969). The frictional behaviour of rock surfaces is affected by composition, surface properties and such external parameters as temperature, absence or presence of water and the state of stress.

Bowden and his co-workers themselves made some experiments on minerals. Bowden (1954) reported results on rock salt in which there was considerable fragmentation of the surface, both on the crystalline and the micro-crystalline scale. Bowden and Tabor (1950, 1964) reported on the significance of contamination on mineral surfaces. For example, for freshly cleaved mica μ was in the order of 1; for a surface which has become contaminated by exposure to the atmosphere μ fell to 0.3; while for a surface which has been outgassed in vacuum, μ rose as high as 35. Horn and Deer (1962) and Penman (1953) measured the coefficient of friction, μ , for different minerals. They concluded that the static coefficient of friction depended upon whether the minerals were massive crystalline such as quartz, feldspars, calcite or laminar such as micas, talc, and clay minerals. They added that up to a critical roughness the coefficient of friction of massive minerals depends upon the amount of water present, water in some cases acting as an anti-lubricant. The laminar minerals, on the other hand,

were lubricated by water in all cases. Some of their results are given in Table (2.1). Concerning the effect of rock type on frictional behaviour, Coulson (1970) studied a variety of rock surfaces and concluded that the frictional behaviour varied with the rock type. On the other hand, Dieterich (1972) conducted double shear tests (Fig. 2.1) and concluded that the frictional behaviour of rock surfaces is determined by surface properties and only weakly related to the rock type. Amadei and Curran (1980) reported that the frictional characteristics of rocks are determined primarily by surface properties and are weakly related to rock type as found by Dieterich (1972). Byerlee (1976) suggested that, for strong brittle rocks such as granite, sliding occurs by brittle fracture of the asperities, but in carbonate rocks such as marble, limestone, etc., plastic deformation occurs at contacting portions of the sliding surfaces.

2.2 THE TIME DEPENDENCE OF FRICTION ON ROCK SURFACES

The length of time that the rock surfaces are held in stationary contact has a significant effect on friction. Rabinowicz (1965) reported that in metals the static coefficient of friction is controlled by the length of time that slip surfaces are held in contact. He found that the coefficient of static friction is proportional to the time of contact according to the following relationship:

$$\mu_s = \mu_D + \alpha t^\beta \quad (\beta < 1) \quad (2.1)$$

with $\mu_D = \gamma/V^\theta \quad (\theta < 1) \quad (2.2)$

Notation: Authors. B, Bowden and Tabor (1950, 1964); By, Byerlee (1967b); H, Hoskins *et al.* (1968); HS, Handin and Stearns (1964); HD, Horn and Deere (1962); J, Jaeger (1959); P, Penman (1953); R, Rae (1963); W, Wiebols *et al.* (1968). l, large surface; s, small surface; t, triaxial test; r, rough surface; g, coarsely ground surface; p, finely ground surface; n, natural shear surface; w, wet surface; c, clean surface.

| Minerals | μ | Minerals | μ | μ (wet) |
|---|-------|-------------------|-------|-------------|
| Na Cl, [B; s] | 0.7 | Quartz, [HD] | 0.11 | 0.42 |
| Pb S, [B; s] | 0.6 | Quartz, [P] | 0.19 | 0.65 |
| S, [B; s] | 0.5 | Feldspar, [HD] | 0.11 | 0.46 |
| Al ₂ O ₃ , [B; s] | 0.4 | Calcite, [HD] | 0.14 | 0.68 |
| Ice, [B; s] | 0.5 | Muscovite, [H, D] | 0.43 | 0.23 |
| Glass, [B; s] | 0.7 | Biotite, [HD] | 0.31 | 0.13 |
| Diamond, [B; s] | 0.1 | Serpentine, [HD] | 0.62 | 0.29 |
| Diamond, [B; s; c] | 0.3 | Talc, [HD] | 0.36 | 0.16 |

| Rocks | μ | Rocks | μ |
|---------------------------|-------|------------------------|-------|
| Sandstone, [R] | 0.68 | Dolomite, [HS; t; g] | 0.4 |
| Sandstone, [J; t; n] | 0.52 | Trachyte, [H; l; p] | 0.63 |
| Sandstone, [H; l; r] | 0.51 | Trachyte, [H; l; g] | 0.68 |
| Sandstone, [H; l; r; w] | 0.61 | Trachyte, [H; l; g; w] | 0.56 |
| Granite, [By; t; n; g] | 0.60 | Marble, [H; l; p] | 0.75 |
| Granite, [By; t; n; g; w] | 0.60 | Marble, [J; t; n] | 0.62 |
| Granite, [H; l; g] | 0.64 | Porphyry, [J; t; n] | 0.86 |
| Quartzite, [W; t; g] | 0.48 | Gneiss, [J; t; n] | 0.71 |
| Quartzite, [W; t; n] | 0.67 | Gneiss, [J; t; n; w] | 0.61 |
| Dolerite, [W; t; g] | 0.64 | Gabbro, [H; l; p] | 0.18 |
| Dolerite, [W; t; n] | 0.95 | Gabbro, [H; l; g] | 0.66 |

Table 2.1 Coefficients of friction of rocks and minerals (Jaeger and Cook, 1979, page 59)

where μ_s and μ_D are the static and dynamic coefficient of friction respectively. α , β , γ , θ are constants for a given set of contact surfaces and t is the time of sticking. V is the sliding speed (Fig. 2.2).

Equation 2.2 shows that the coefficient of sliding friction μ_D decreases as sliding speed increases. Similar results were obtained by Miller (1962) as illustrated in Fig. (2.3).

Dieterich (1972) investigated the time dependency of rock friction using clean rough and ground surfaces of sandstone, quartzite, graywacke and granite in a range of 2-85 MPa normal stress and over a range of time of $1-10^5$ seconds, (Fig. 2.4), using a double shear apparatus (Fig. 2.1). He used two extremes in surface finish. Smooth and rough surfaces were prepared by lapping with # 600 and # 80 silicon carbide abrasive respectively. He concluded that frictional characteristics of rock surfaces is determined primarily by surface finishing and only weakly related to the type of rock. He also derived the following expression between the static coefficient of friction μ_s and time of sticking t in seconds:

$$\mu_s = \mu_0 + A \log t \quad (2.3)$$

where μ_0 is the initial coefficient of friction and A is a constant. In a later paper Dieterich (1978) revised equation 2.3 to:

$$\mu_s = \mu_0 + A \log (\beta t + 1) \quad (2.4)$$

where β is constant.

Dieterich (1972) observed time-dependency only for the rough-ground surfaces that were separated by a thin layer of displacement-produced wear particles. Studies by Scholz and Engelder (1976), Engelder and Scholz (1976) and Teufel and Logan (1977), on

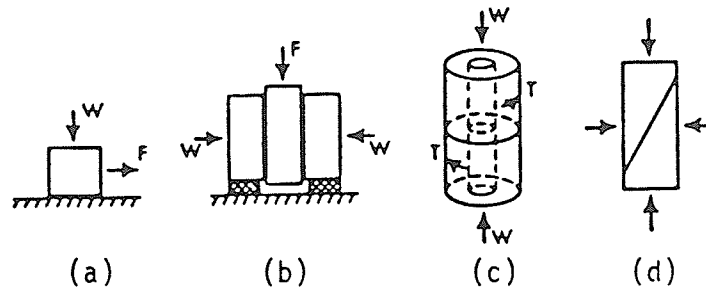


Fig. 2.1 Different devices used to determine the frictional properties of rock surfaces.

- a) The surfaces are pressed together by normal force W
- b) Double shear tests (one block pushed between others)
- c) The rotating system
- d) Sliding across inclined surfaces in a cylindrical specimen (Jaeger and Cook, 1979, page 58)

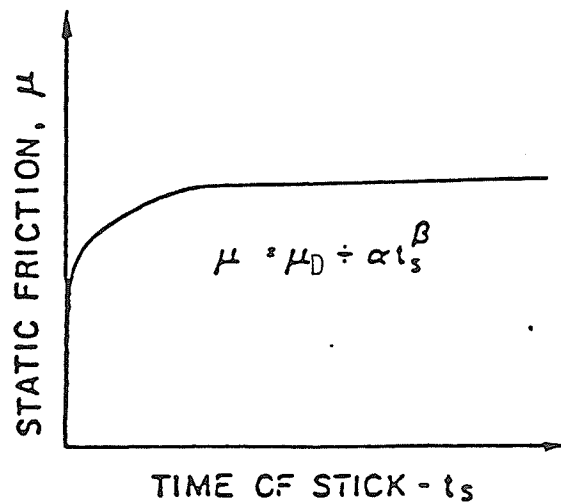


Fig. 2.2 Typical relationship between static friction and time of stick (Rabinowicz, 1965)

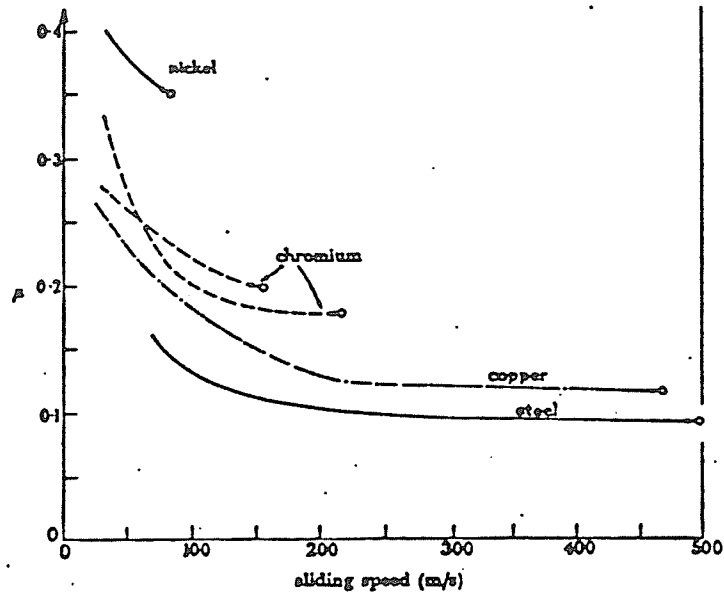


Fig. 2.3 Influence of sliding speed on coefficient of friction for steel, copper, chromium and nickel sliding on sapphire (Miller, 1962)

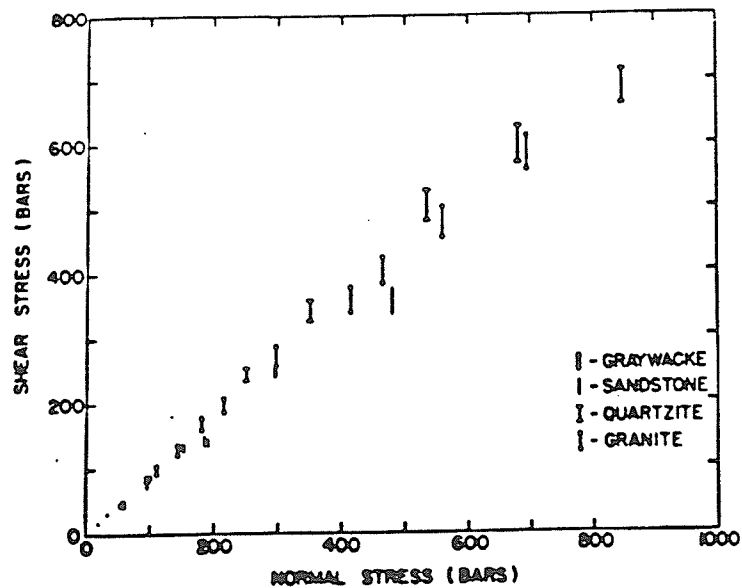


Fig. 2.4 Summary of experimental results. The lower end of each bar gives the shear strength for 15-sec stick intervals; the upper end of the bar gives the strength for 10³-sec stick intervals (Dieterich, 1972)

the other hand, show that the time dependent increase in the static coefficient of friction is a general characteristic of rock friction under a variety of test conditions and slip surface properties.

B. Amadei and J.H. Curran (1979) carried out a number of experiments to investigate the time-dependency of friction. Five saw-cut samples of different rock types were studied in order to see if the rock type has any influence on the time-dependence of rock friction. These were creep tests, where the normal and shear stresses were maintained constant during the tests. They concluded that the coefficient of static friction increases with the logarithm of the time of sticking according to the relations 2.3 and 2.4 found by Dieterich (1972, 1978). They also concluded that the time-dependent increase in static friction is a general characteristic of rock friction. They added that the frictional characteristics of rocks are determined primarily by surface properties and are weakly related to rock type as found by Dieterich (1972).

2.2.1 Mechanism of Time-Dependency

Different mechanisms have been proposed to explain the time-dependence of the static coefficient of friction. Dieterich (1978) discussed the mechanisms and reported that the similarity of the increase of the coefficient of static friction for both metals and rocks with time suggests that the same mechanism that was proposed by Bowden and Tabor (1964) for metals is applicable to rock friction. Bowden and Tabor actually (1964) proposed two possible mechanisms:

1. A mechanical mechanism, where the area of adhesive contacts between the surfaces increases because of localized creep.

2. A chemical mechanism, where the area of adhesive contacts remains constant with time, but the strength of the contacts increases because of time-dependent breakdown of surface films that interfere with adhesion.

Dieterich (1972) suggested the first mechanism proposed by Bowden and Tabor (1964) to be the more important, but he did not eliminate the possibility of the second mechanism. Similarly, Scholz et al. (1972) suggested increase of contact area by creep at points of contact as the mechanism of time-dependent friction. Byerlee (1967) concluded that surface conditions change with time because the asperities on the surface may lock and then fail through brittle fracture. Teufel and Logan (1977) conducted a series of experiments on sawcuts sandstone and measured the area of true contact at different displacement rates. Their results show that the contact area increases with decreasing displacement rate.

2.3 STICK-SLIP PHENOMENA

Frictional sliding between finely ground or polished rock or metal surfaces is sometimes accompanied by severe vibrations. This is known as stick-slip (Bowden and Leben, 1939).

Most of the research on stick-slip has been with metals. Bowden and Leben (1939) attributed stick-slip to the sudden slips after welded junctions failed. Based on his observations of friction in metals (Rabinowicz, 1965), reported that if static coefficient of friction exceeds sliding coefficient of friction, stick-slip instability will occur, otherwise stable sliding takes place.

As far as stick-slip on rock surfaces is concerned, several

authors tried to understand the conditions under which it occurs. However, there is little agreement among the different authors. Hoskins, Jaeger and Rosengren (1968) observed stick-slip only with smooth surfaces. Jaeger (1959) observed them with ground surfaces, but not with natural surfaces. On the other hand, Brace and Byerlee (1966) described stick-slip as occurring in both cases and later (1968) they found that confining pressure and rock type are the most important parameters to control the mode of sliding and they added that strain rate has no influence on stick-slip.

Teufel and Logan (1978) reported that "In our experiments, as the nominal displacement rate decreases, there is a transition in mode from stable sliding to stick-slip. With a further decrease in this rate the magnitude of the stick-slip events increases." Byerlee (1967a) reported that stick-slip is more pronounced for rough than smooth surfaces. Engelder and Scholz (1976) proposed two processes to explain stick-slip instability, one is ploughing of the asperities, and the other is creep at points of contact of the sliding surfaces. Concerning the normal stress and the rock type dependency on stick-slip, Coulson (1970) found that stick-slip occurred within a wide range of normal stresses in several rock types in a direct shear test. Dieterich (1972) examined different kinds of rocks using different normal stresses. He found that sliding on clean rough-ground surfaces was initially stable, however, as rock debris accumulated on the surfaces, stick-slip become the dominant mode of sliding.

Byerlee (1970) thought that irregularities of the surfaces are the cause of stick-slip. During slip these irregularities become locked, movement stops then resumes after they fail by brittle fracture.

Teufel and Logan (1978) summarized the mechanisms which can account for the instability required for stick-slip as (a) brittle fracture, (b) creep, and (c) local melting. They added that the relative importance of these mechanisms depends on not only the properties of the particular material but also the environmental conditions of effective confining pressure and surrounding temperature. And, finally, Jaeger (1979) described stick-slip as a complex phenomenon that can be caused by many factors such as surface roughness, time between sliding, rate of sliding and gouge accumulation. To this one may add the influence of the testing system itself, and in particular the reaction time involved while the hydraulic loading system adjusts to the conditions created by a sudden stick-slip effect.

CHAPTER 3

TESTING EQUIPMENT AND SET UP

The chief objective of the experiments was to define the time dependence of the frictional resistance developing on a flat, macroscopically smooth and worn discontinuity in Lac du Bonnet granite. The secondary objective was to gain some insight into the nature of the mechanism causing the time effect. The latter was to be reached by continuously measuring the four parameters of the direct shear test: the normal and shear loads and the normal and shear displacements.

3.1 TEST SPECIMEN

3.1.1 Rock Type

The rock type used in this testing program was Lac du Bonnet (LDB) granite. It was extracted and obtained from the Cold Spring Quarry, Manitoba, located within the Lac du Bonnet Batholith (Fig. 3.1). Tammemagi et al. (1979) described the Batholith as a shallow, sheet-like granite intrusion, covering an area of over 1,000 km², located southeast of Lake Winnipeg on the western edge of the exposed Canadian Shield.

In general, LDB granite is an acidic granular rock, medium to coarse grained (0.5 mm - 20 mm), pink and homogeneous, consisting of feldspar, quartz and mica. It may contain a little dark mineral (not more than 5-10%), commonly hornblende and biotite. The specific gravity of granite ranges from 2.54 to 2.78. According to Lajtai (1981), the LDB granite is composed of quartz ($\approx 30\%$), microcline (\approx

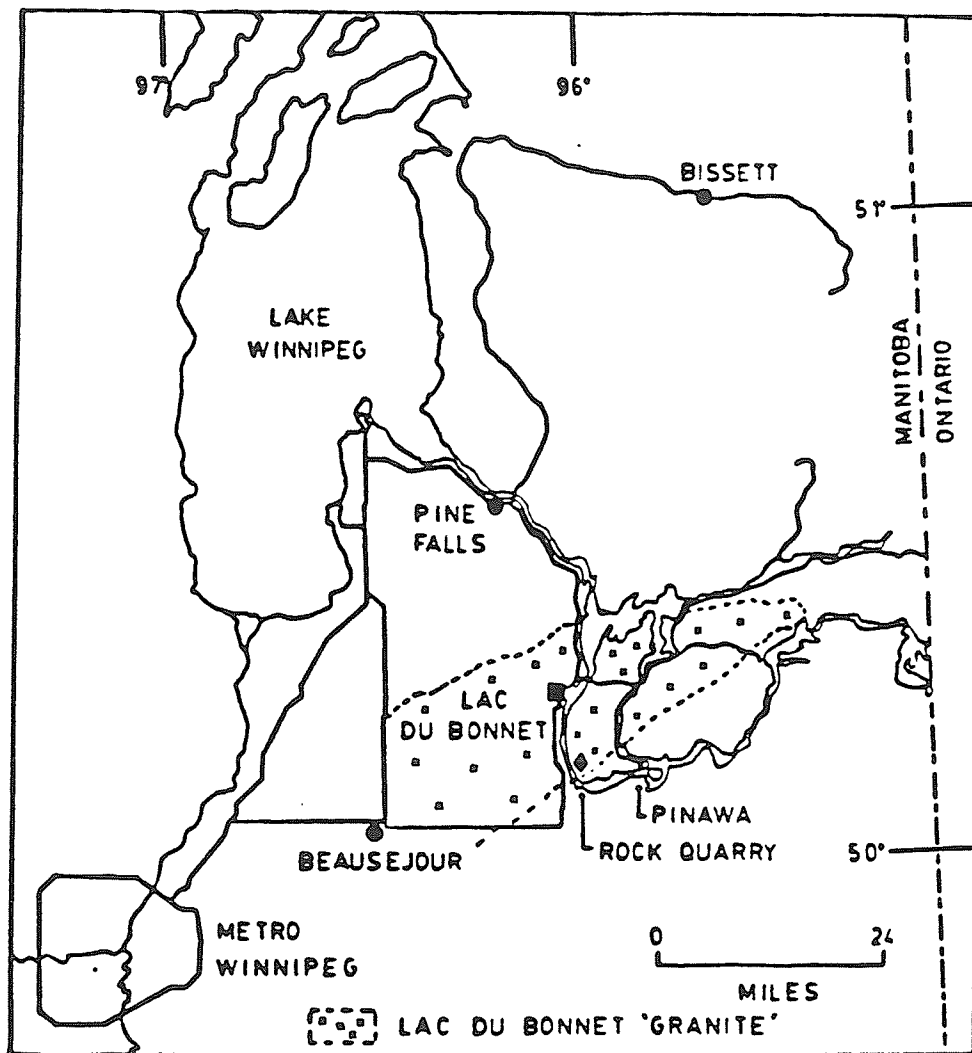


Fig. 3.1 Location map

30%), oligoclase ($\approx 35\%$), and biotite ($\approx 5\%$).

3.1.2 Selection and Preparation of Test Specimens

The specimens tested were obtained from the same single block in order to avoid variation in strength from specimen to specimen in one particular type of testing, and for comparison of results.

All specimens were cut with a diamond saw to the approximate dimensions that should fit into the shear box machine. The upper and the lower boxes were cylindrical in shape with a diameter of 12.70 cm and height of 6.4 cm. It is very difficult and even impossible to produce a round sample from granite to fit into the boxes. However, the boxes were modified to a square shape using steel plates in each box. After modification, the upper and lower area of the boxes became 8.9 cm x 8.9 cm.

The lower block specimen was sawn to an approximate dimension of 8.9 cm x 8.9 cm x 6.4 cm, while the upper one was 3.9 cm x 8 cm x 6.4 cm. This made the upper surface of the test specimen smaller than the lower surface to avoid any change of the apparent area of contact with movement. The specimens then were grounded to bring them to final size. This ensured a snug fit in the shear boxes and provided flat surfaces for seating and loading of the samples. At the bottom of the lower sample, a piece of steel, having the same dimensions as the lower sample surface, was placed to raise the sample to provide a 3 mm clearance between the upper and lower shear boxes (Fig. 3.2a).

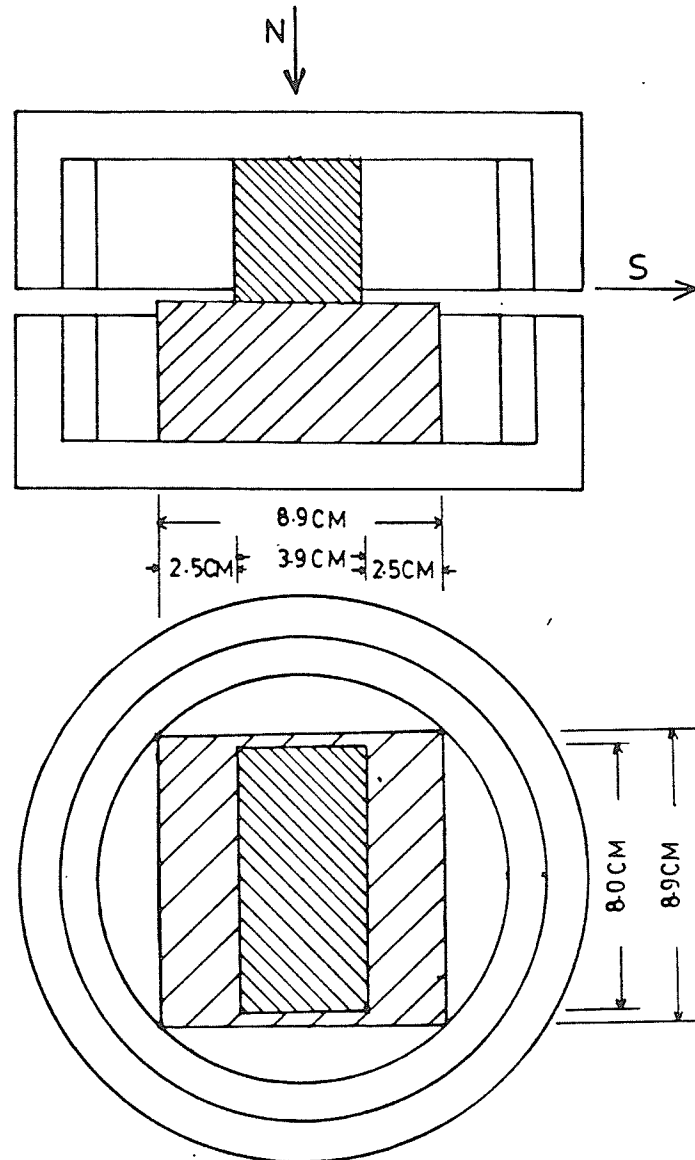


Fig. 3.2a Schematic view of the sample arrangement in direct shear box. The test specimen is shaded

3.2 TESTING EQUIPMENT AND SET UP

3.2.1 Direct Shear Machine

A RM 101 direct shear machine was used for this testing program. The machine was manufactured by the Structural Behaviour Engineering Laboratories, Inc. The detailed arrangement of the direct shear machine is illustrated in Fig. 3.2b.

3.2.2 Normal and Shear Loading RAMs

RAMs RC-151 and RCH-121, manufactured by ENERPAC, were used for normal and shear loading respectively. The normal RAM has an effective area and maximum capability of 20.26 cm² and 15 tons respectively, while the shear RAM has 12.18 cm² and 12 tons. The normal RAM was connected to a pressure supply by means of a hydraulic hand pump. In case of shear, loading was through an air-hydraulic booster assembly (Fig. 3.3).

3.2.3 Transducers

Two pressure transducers were used to measure normal and shear loads. For displacement measurements, three HP7DCDT LVDTs (linear variable differential transducer) were used. Two read the vertical, and one the horizontal displacement.

3.3 CALIBRATION OF PRESSURE AND LVDT TRANSDUCERS

The pressure transducer in the normal loading system was calibrated using a universal testing machine. The calibration was done for a range of normal load from 0 to 45 kN (Fig. 3.4). The same machine and load range was used for the shear load calibration (Fig.

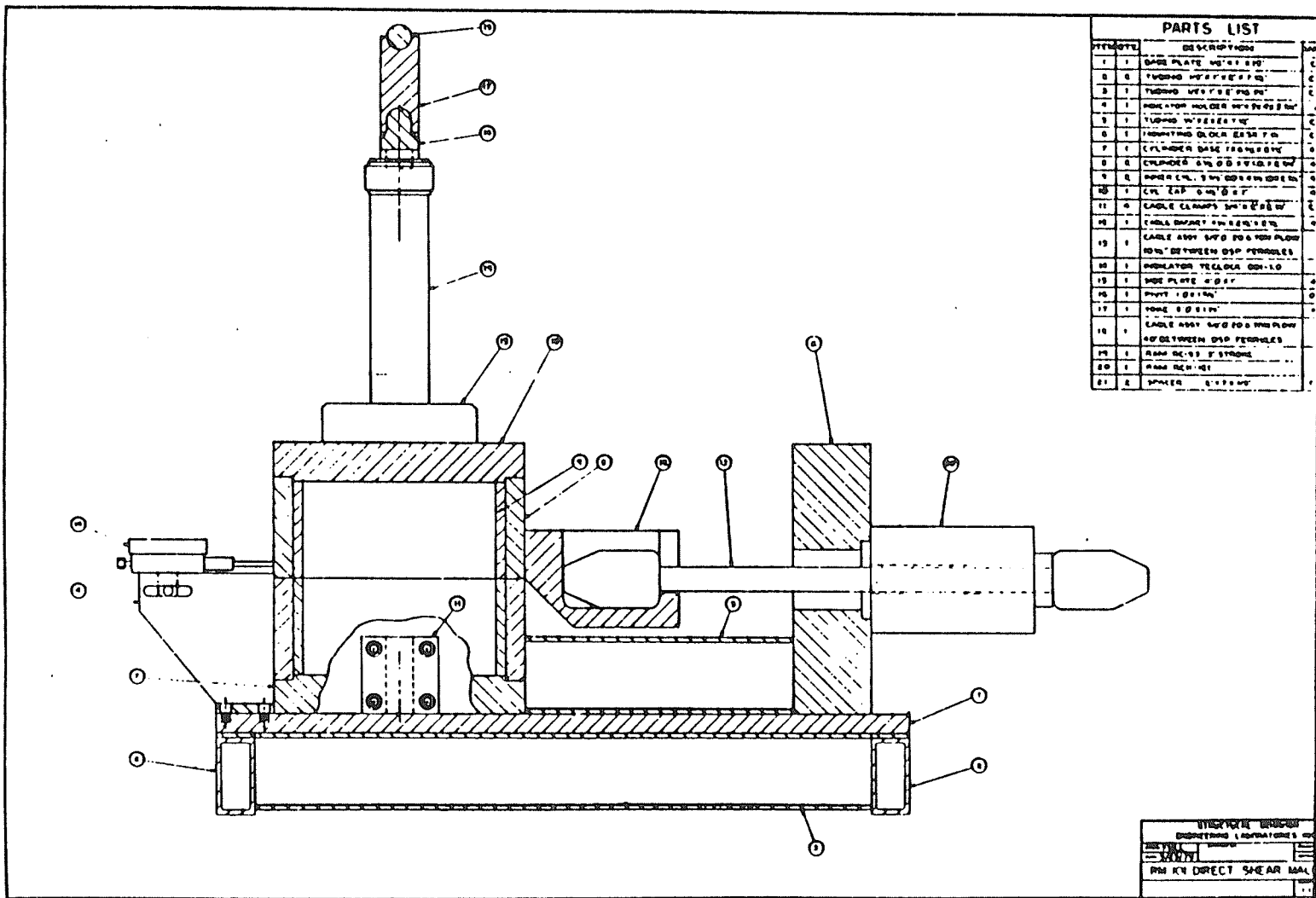


Fig. 3.2b SBEL direct shear machine

3.5).

The horizontal and vertical displacements were measured by using LVDT transducers. These transducers were calibrated by using a micrometer calibrator. The calibration curves are presented in (Fig. 3.6) and (Fig. 3.7) respectively.

3.4 FINAL SET UP

After the calibration, the experimental set up was completed by connecting all LVDTs and pressure transducers to an automatic data acquisition system, HP Model 3054A connected to an HP micro computer, Series 200, Model 16.

3.5 SHEAR LOAD CORRECTION

The shear machine is constructed in such a way that the normal load has a shear component. This component becomes greater as displacement progresses. A correction of the shear load therefore was necessary. This can be expressed in Fig. 3.8, where the true shear load decreases with horizontal displacement causing anti-shear load of the amount:

$$S_A = [\text{SIN} (\text{TAN}^{-1} (\text{DISP}/475000))] \times N$$

This amount was subtracted from the measured shear load at every reading using a computer sub-program in later analysis; an example of this correction is given in Fig. 3.9. The displacement for this correction is entered in micrometers.

It should be noted here that the normal load was not corrected because the correction was too small when compared with the statistical variation in normal load during the test.

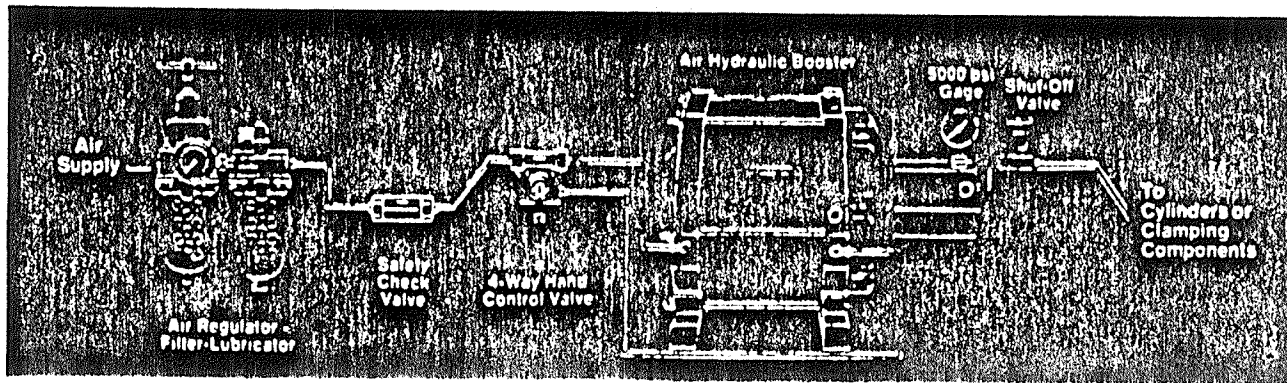


Fig. 3.3 ENERPAC air hydraulic booster system

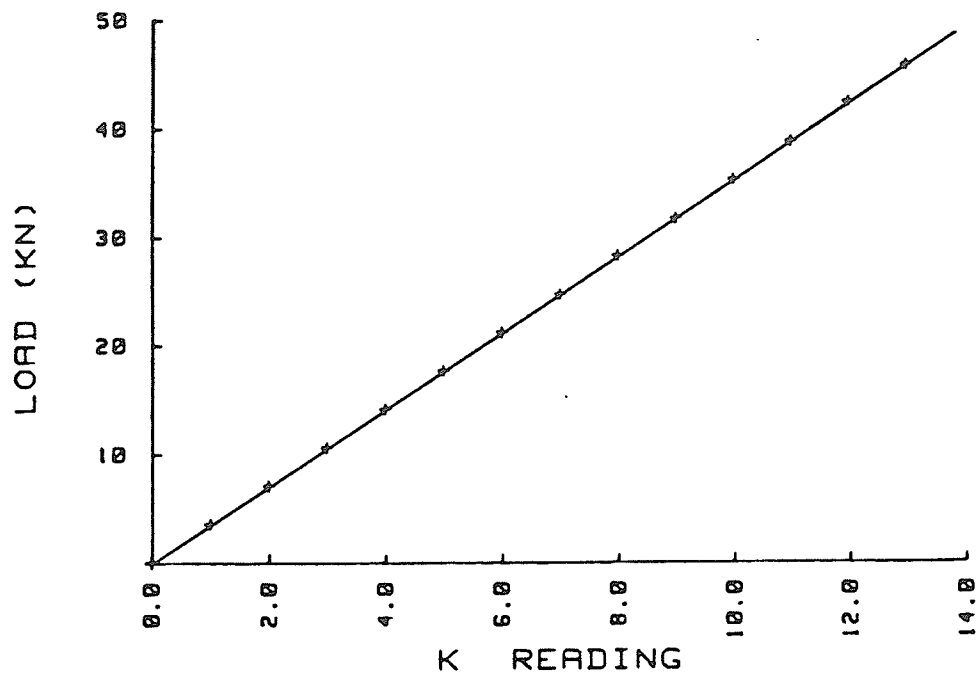


Fig. 3.4 The calibration curve for the normal load reading (K READING) on the Kaye Data Acquisition System

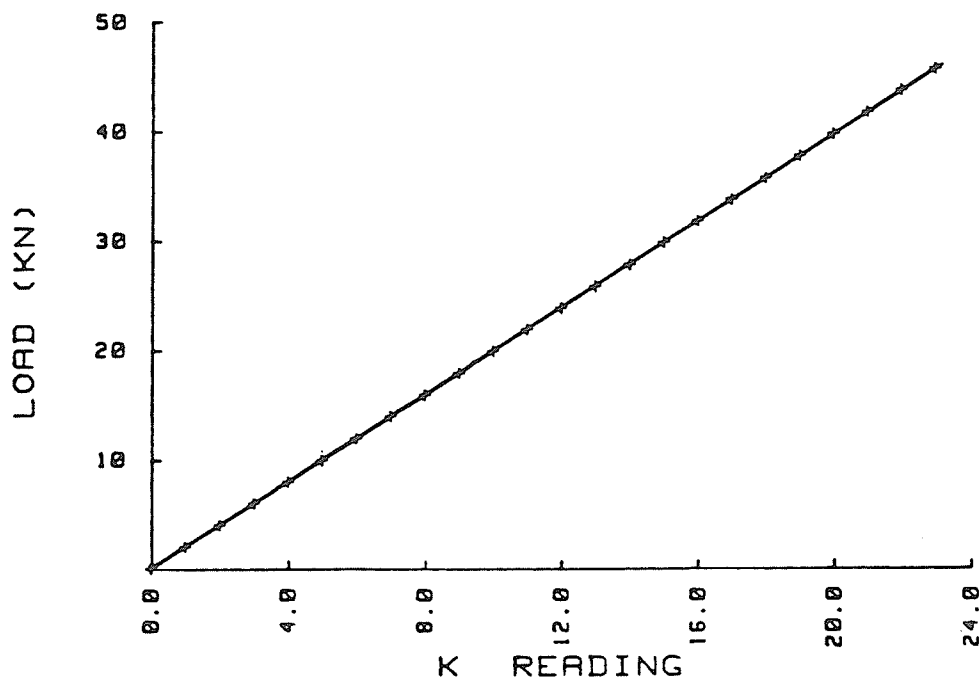


Fig 3.5 The calibration curve for the shear load reading (K READING) on the Kaye Data Acquisition System

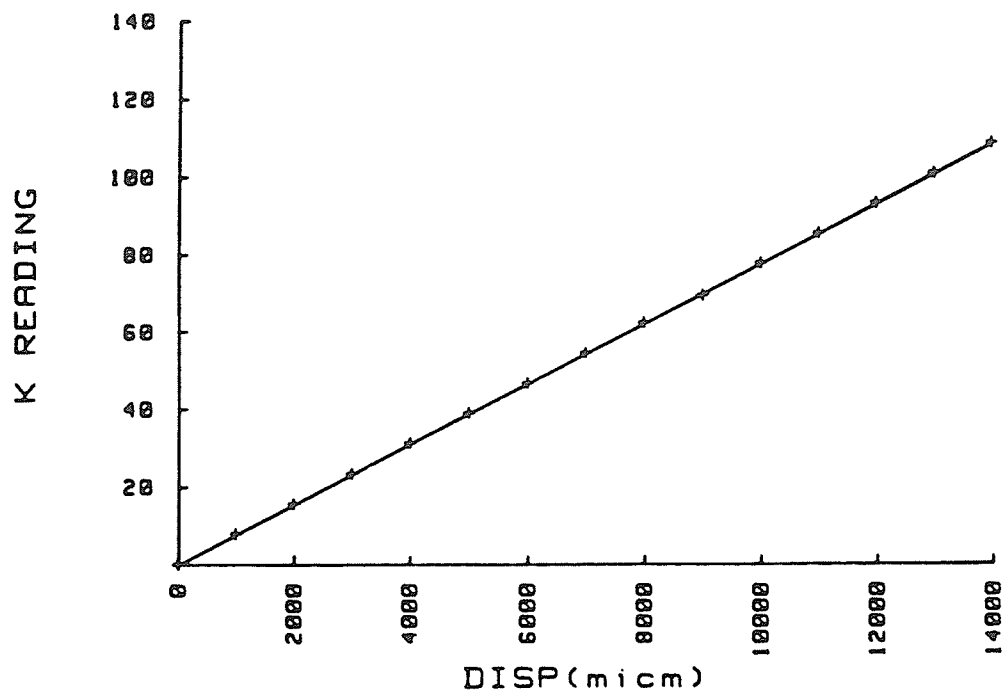


Fig. 3.6 The calibration curve for the horizontal displacement reading (K READING) on the Kaye Data Acquisition System

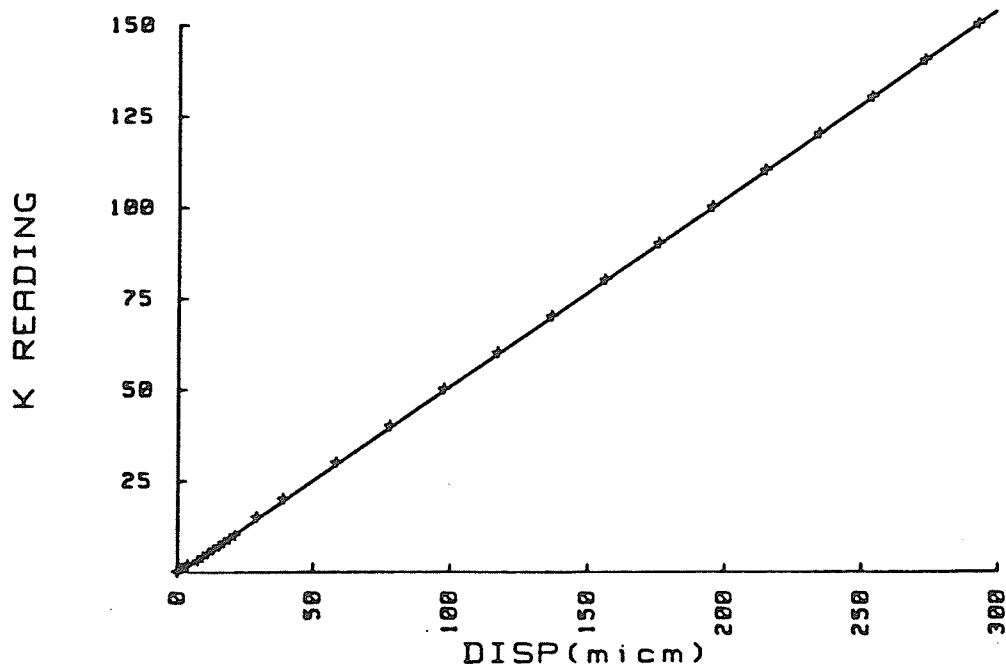


Fig. 3.7 The calibration curve for the vertical displacement reading (K READING) on the Kaye Data Acquisition System

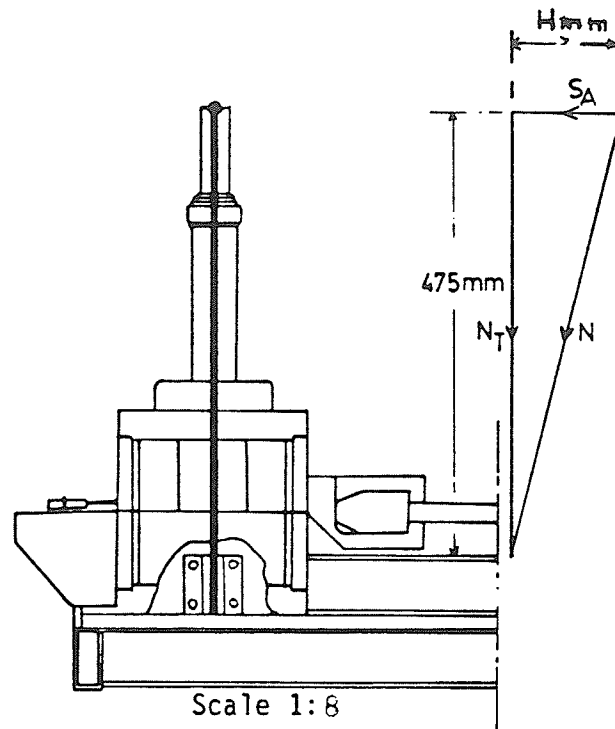


Fig. 3.8 Illustration of the shear load correction. The amount S_A was subtracted from the shear load reading. H is the shear displacement

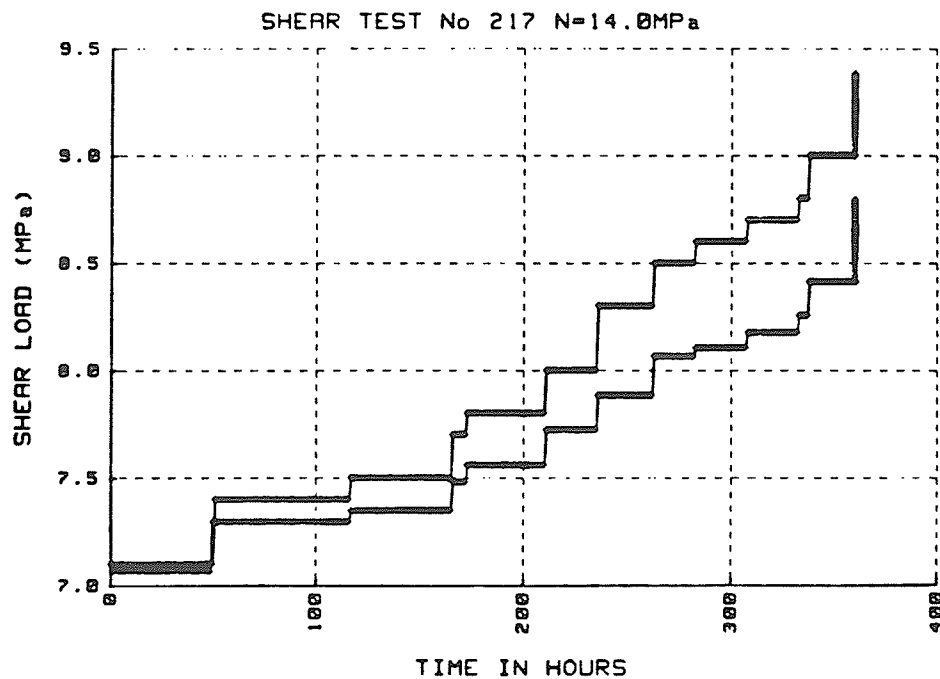


Fig. 3.9 An example for the shear load correction. Top curve is recorded and bottom curve is the corrected shear load

CHAPTER 4

LABORATORY INVESTIGATION

4.1 BASIC FRICTION ANGLE ϕ_b

In order to evaluate the frictional resistance of a discontinuity, the "basic friction angle ϕ_b " must first be determined with the direct shear machine using a flat artificially prepared surface (Barton, 1971). As far as the surface preparation for determining the angle of basic friction is concerned, different types of surface finishing were suggested in the literature. Rough sawn rock surfaces were suggested by Patton (1961), whereas Barton (1971) used surfaces prepared by a sandblasting technique and Coulson (1972) employed surfaces prepared with # 80 grit (silicon carbide grits). Dieterich (1972) used # 600 grit for smooth surfaces and # 80 grit for rough surfaces. Clearly, whatever the preparation technique is, the result will be an artificial surface that bears little relationship to natural surfaces.

In this study, the intact samples were cut with a diamond saw as described earlier (Section 3.1.2) and then finished by lapping with number 40 grit sand paper. The basic friction angle for this surface was found by doing both direct shear and tilt-table tests.

4.1.1 Direct Shear Test

The procedure for the determination of the basic friction angle using the direct shear test was as follows:

The specimen was positioned in the shear box. The normal load was first applied to the desired value ranging between 1-15 MPa.

Shear load was then applied until the first slip occurred. After that the specimen was removed from the shear box, the surface was cleaned and polished with # 40 grit. The specimen was then repositioned and the test repeated in the same manner.

Fig. (4.1) gives a typical load-displacement curve which resulted from this procedure, while Fig. (4.2) shows the dependence of the shear load at first slip on the magnitude of the normal load. The slope of the linear regression line is the coefficient of friction ($\mu = .45$) corresponding to an angle of friction of 24° .

4.1.2 Tilt Table Test

The direct shear tests used a relatively large normal load. It was desirable to repeat the experiments with a much smaller normal load. This is best accomplished with the tilt table test. The tilt table tests were conducted at a normal load of .002 MPa (normal component of the weight of the block). The tilt table apparatus is a simple friction apparatus, described in detail by Bruce (1978). The sample is positioned with the bottom half clamped on the plane while the top half is subjected to slide relative to the bottom half when the plane is tilted. The angle of tilt when movement starts is the angle of friction. The same specimen with the previously described surface finishing was used. The average value from 9 tests was 23° with a range of 21 to 24° , that is slightly lower than the value obtained at the higher normal load of the direct shear tests.

4.2 THE INFLUENCE OF LOADING RATE ON THE FRICTIONAL RESISTANCE

The displacement rate has been shown to have an influence

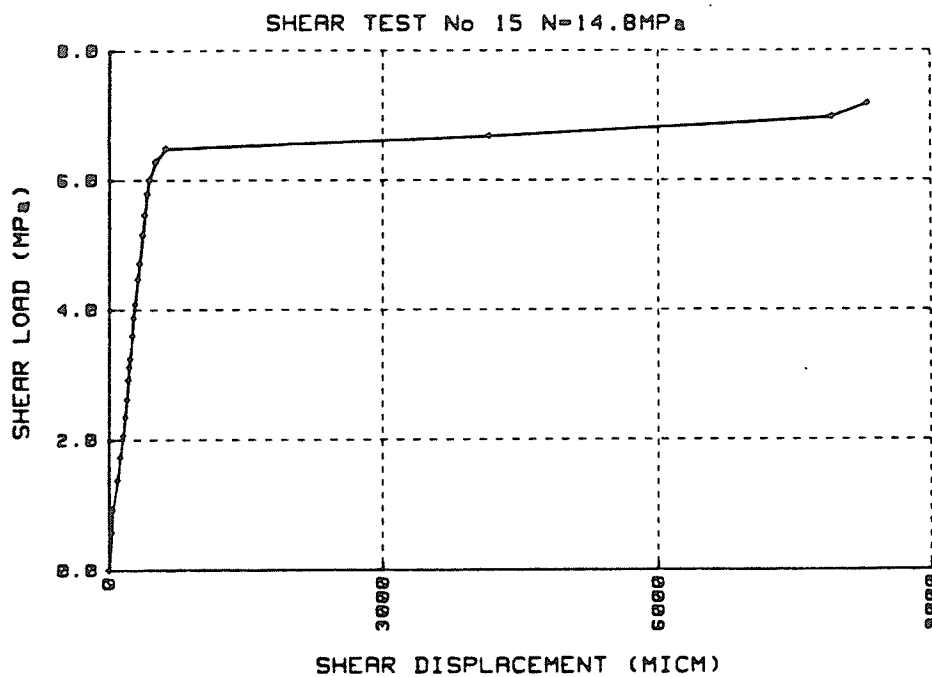


Fig. 4.1 A typical load displacement curve for loading to first slip

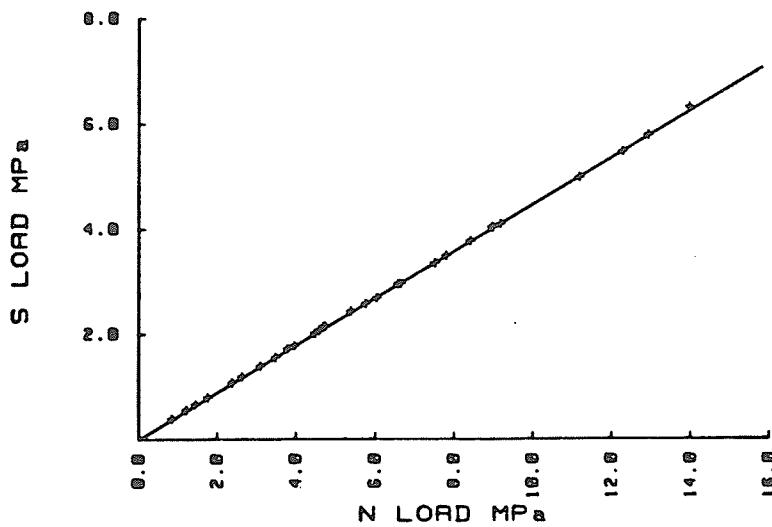


Fig. 4.2 The relationship between shear load at first slip and the normal load. The surface is flat, ground with # 40 grit

on the measured friction angle (Teufel and Logan, 1978). To investigate this, 4 test series, each at a different normal load, were conducted. Within a single series the shearing load rate was varied.

At this stage it was decided to change the surface characteristics. Clearly the surface finish has a great influence on the friction angle. To compare results from tests to tests, standardization is necessary. However, it was felt that a standard grit finish bears little resemblance to natural surfaces. Therefore in all the following tests a "worn" surface was used. This was prepared by repeated (about 100 times) shear test runs. The resulting surface had shown some wear and some slickensiding. It should compare with natural surfaces that have undergone shear displacement in nature.

Experiments were conducted at normal loads 4, 5, 6 and 14 MPa. Once the normal load was reached, shear loading followed in short order. The shear loading rate was manually controlled and ranged from 5.55×10^{-6} to 0.7 MPa/sec (Table 4.1). The shear load listed in the Table represents the load at first slip.

In general, the lower the loading rate is, the higher the frictional resistance becomes.

In the investigated range of loading rates (5.56×10^{-6} - 0.7 MPa/s), the obtained friction angle varied between 19 and 31 degrees.

TABLE 4.1 The influence of loading rate on
the frictional resistance

| EXP. No. | N. Load MPa | Loading Rate MPa/sec | S. Load MPa | ϕ degrees |
|----------|----------------|-------------------------|----------------|-------------------|
| 179 | 4.0 | 8.59×10^{-6} | 1.7 | 23.0 |
| 182 | 4.0 | 8.59×10^{-6} | 1.7 | 23.0 |
| 180 | 4.0 | 5.56×10^{-6} | 2.3 | 29.9 |
| 109 | 5.0 | 1.13×10^{-1} | 1.7 | 18.8 |
| 199 | 5.0 | 5.26×10^{-2} | 2.0 | 21.8 |
| 110 | 5.0 | 2.00×10^{-2} | 2.4 | 25.6 |
| 111 | 5.0 | 1.88×10^{-2} | 2.6 | 27.5 |
| 202 | 5.0 | 3.84×10^{-3} | 3.0 | 31.0 |
| 112 | 6.0 | 8.48×10^{-2} | 2.8 | 25.0 |
| 113 | 6.0 | 2.90×10^{-2} | 2.9 | 25.8 |
| 114 | 6.0 | 1.62×10^{-2} | 3.4 | 29.5 |
| 174 | 14.0 | 7.00×10^{-1} | 5.6 | 21.8 |
| 169 | 14.0 | 1.30×10^{-1} | 6.5 | 25.0 |
| 165 | 14.0 | 1.15×10^{-1} | 6.9 | 26.3 |
| 170 | 14.0 | 6.02×10^{-2} | 7.1 | 26.9 |
| 172 | 14.0 | 1.65×10^{-2} | 7.3 | 27.6 |

CHAPTER 5

LABORATORY INVESTIGATION OF THE TIME-DEPENDENCY OF FRICTION

The friction angles determined in all previous tests were those representing conditions at first slip. It was found however, that after first slip, the shear load had to be increased above that at first slip to cause continuing displacement. The cause of this behaviour is investigated in this chapter.

5.1 EFFECT OF NORMAL LOAD HISTORY ON THE STATIC COEFFICIENT OF FRICTION

In the first series of experiments, the dependence of the friction angle on the time of normal load application (in the absence of shear load) was investigated.

Specimen preparation and set up for testing were described in Chapter 3. The shear surface of the test specimen was polished using # 40 grit. Experiments were then conducted at the constant normal load of 4.6 MPa. To determine if the static coefficient of friction changed with time, the duration of stick was varied by holding the normal load constant for different time increments; ranging from 0 to 100 hours. At the end of each desired time interval, the shear load was rapidly applied (about 1 second) until first slip occurred. At the end of each experiment the same surface was repolished using the same grit number and the test repeated at the same constant normal load but a different stick interval.

The results are summarized in Table 5.1. It is of interest to notice from this Table that under a constant normal load the coefficient of static friction increased from 0.447 ($\phi = 24.1^\circ$) at

TABLE 5.1 Influence of sticking time

| Time Hours | Shear (MPa) | Coef. St. Fr. | Fric. Angle |
|------------|-------------|---------------|-------------|
| 0.0 | 2.056 | .447 | 24.1 |
| 0.0 | 2.052 | .446 | 24.0 |
| 0.0 | 2.056 | .447 | 24.1 |
| 1.0 | 2.065 | .449 | 24.1 |
| 3.0 | 2.075 | .451 | 24.3 |
| 6.0 | 2.084 | .453 | 24.4 |
| 12.0 | 2.116 | .460 | 24.7 |
| 15.0 | 2.125 | .462 | 24.8 |
| 18.0 | 2.139 | .465 | 24.9 |
| 20.0 | 2.148 | .467 | 25.0 |
| 24.0 | 2.167 | .471 | 25.2 |
| 24.0 | 2.163 | .470 | 25.2 |
| 24.0 | 2.165 | .471 | 25.2 |
| 24.0 | 2.165 | .271 | 25.2 |
| 30.0 | 2.190 | .476 | 25.4 |
| 38.0 | 2.224 | .483 | 25.8 |
| 40.0 | 2.236 | .486 | 25.9 |
| 46.0 | 2.263 | .492 | 26.2 |
| 50.0 | 2.282 | .496 | 26.4 |
| 58.0 | 2.314 | .503 | 26.7 |
| 62.0 | 2.337 | .508 | 26.9 |
| 68.0 | 2.360 | .513 | 27.2 |
| 72.0 | 2.374 | .516 | 27.3 |
| 72.0 | 2.378 | .517 | 27.3 |
| 72.0 | 2.372 | .516 | 27.3 |
| 75.0 | 2.387 | .519 | 27.4 |
| 80.0 | 2.410 | .524 | 27.7 |
| 86.0 | 2.433 | .529 | 27.9 |
| 90.0 | 2.456 | .534 | 28.1 |
| 96.0 | 2.479 | .539 | 28.3 |
| 100.0 | 2.493 | .542 | 28.5 |
| 100.0 | 2.498 | .543 | 28.5 |

instant shearing (about 5 seconds) to 0.543 ($\phi = 28.5^\circ$) after 100 hours stick duration. Accordingly the frictional resistance increased from 2.056 MPa to 2.497 MPa.

Figs. (5.1) and (5.2) show the relation between the time of sticking and static coefficient of friction. The collected data fit the equation:

$$\mu_t = \mu_0 + \gamma t$$

where μ_t is the static coefficient of friction at t normal-stick duration in hours, μ_0 is the static coefficient of friction at time < 5 sec and γ is a constant = 9.2336×10^{-4} . Although a straight-line relationship fits the data well for the 0 to 100 hour range, it is likely that an investigation involving longer periods of "sticking" time would find that the rate of increase diminishes with time and perhaps approaches an asymptote.

It should be noted here that the results obtained by Dieterich (1972) and Amadei (1979) on the time dependence of the static coefficient of friction were with tests performed under constant normal and shear loads, where the shear load was held constant slightly below the peak strength. In this study only the normal load was held constant and no shear load was applied.

5.2 LONG-TERM STRENGTH ALONG THE DISCONTINUITY

In this series of tests the goal was to find out how high the shear load can be increased when time is allowed between shear load increments. The tests may be considered as equivalent to incremented load creep tests. During the test all the direct shear parameters (shear load, normal load, shear displacement and dilation)

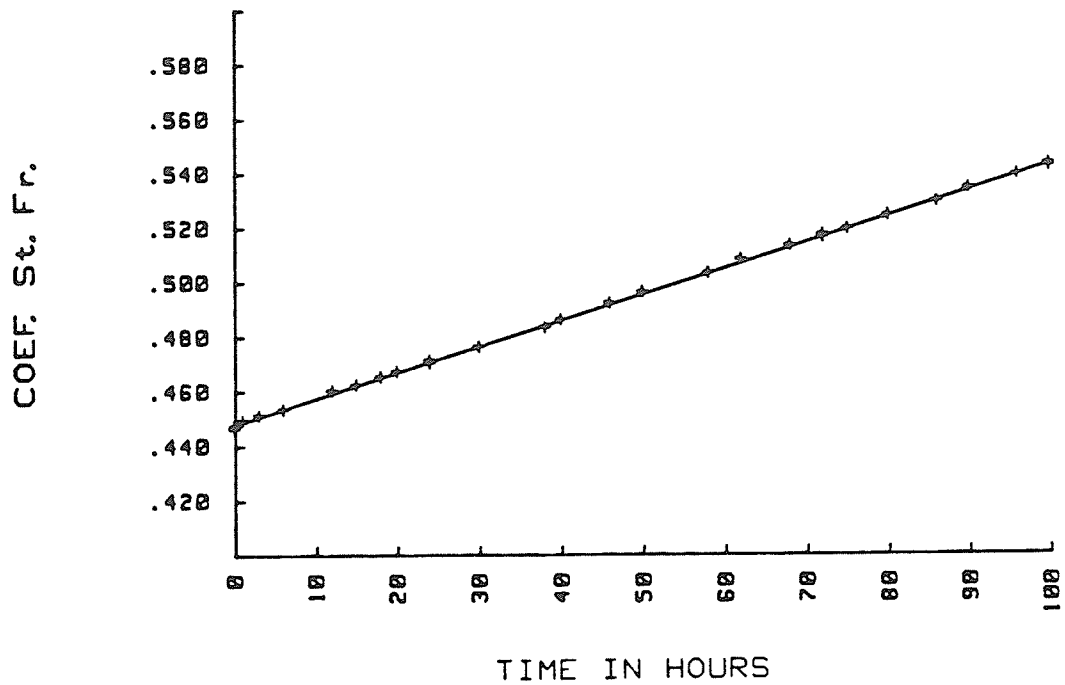


Fig. 5.1 The influence of the "sticking time" on the coefficient of friction. The surface is flat, ground with # 40 grit

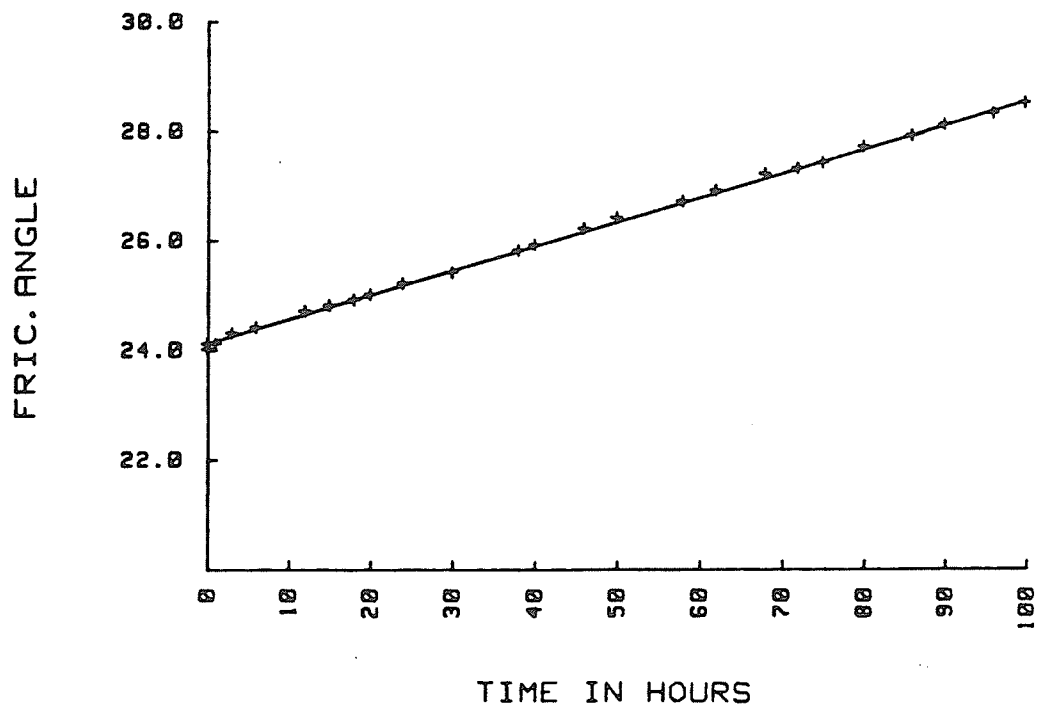


Fig. 5.2 The influence of "sticking time" on the angle of friction. The surface is flat, ground with # 40 grit

were recorded for later analysis. The shear surface of each test specimen was prepared as indicated in Section 4.4.

In each test, the normal load was first applied and kept constant within $\pm 5\%$. The shear load was then slowly increased until the first slip was observed, at which time shear loading was halted. Once movement along the surface ceased, the shear load was incremented. Altogether 2.5 cm displacement could be accommodated within the testing arrangement. Approximately 4 to 10 increments could be applied within these limits. On reaching a displacement of 2.5 cm, the test was terminated and the specimen repositioned for the new test. Duration of 2 complete tests (0 to 2.5 cm of displacement) was varied from 20 min to 15 days. The results are summarized in Table 5.2. For three tests (1957, $N = 1.5$ MPa; 127, $N = 9.0$ MPa; 217, $N = 14.0$ MPa) results are presented in detail in Table (5.3a,b,c). Fig. (5.3a,b,c) show the variation of displacement with time for the same tests.

5.3 DESCRIPTION OF THE SHAPE OF LOAD AND DISPLACEMENT CURVES

In all tests, both loads and the horizontal and vertical displacements were recorded. From the data, load versus displacement, displacement versus time (creep curve), and load versus time, plots were prepared. Individual features of these curves are as follows:

1. During the normal load application (Fig. 5.4), the displacement versus time curves show closure in the direction of the normal load (Fig. 5.5) and usually some reverse movement along the shear direction (Fig. 5.6).
2. When the shear load was increased (Fig. 5.7), there was

TABLE 5.2 Friction on worn granite surfaces

| Exp. No. | Normal Load MPa | Shear Load at 1st Slip MPa | Disp. at 1st Slip mm | Friction Angle ϕ_1 at 1st Slip | Shear (S), Disp (δ) and ϕ_2 at time t | | | | |
|----------|--------------------|----------------------------------|----------------------------|---|---|----------------|-------------|-----------------|-------------------|
| | | | | | S MPa | ϕ_2° | δ mm | Time t hours | $\phi_2 - \phi_1$ |
| 127 | 9.0 | 4.0 | 0.19 | 23.5 | 4.80 | 28.0 | 12.7 | 336.0 | 4.5 |
| 163 | 12.4 | 6.9 | 8.50 | 29.0 | 7.45 | 31.0 | 7.0 | 3.5 | 2.0 |
| 164 | 12.5 | 7.0 | 5.50 | 29.3 | 7.50 | 31.0 | 8.0 | 0.4 | 1.7 |
| 167 | 12.9 | 8.0 | 0.75 | 31.8 | 8.38 | 33.0 | 24.0 | 150.0 | 1.2 |
| 1757 | 14.0 | 7.5 | 0.75 | 28.2 | 8.08 | 30.0 | 4.6 | 1.0 | 1.9 |
| 179-180 | 4.0 | 1.7 | 1.00 | 23.0 | 2.30 | 29.9 | 7.0 | 170.0 | 6.9 |
| 181 | 6.8 | 2.4 | 2.00 | 19.5 | 3.13 | 24.7 | 12.5 | 182.0 | 5.2 |
| 182 | 4.5 | 1.6 | 0.56 | 19.6 | 2.21 | 26.0 | 22.2 | 168.0 | 6.4 |
| 183 | 2.6 | 1.4 | 0.60 | 28.3 | 1.44 | 29.0 | 1.6 | 1.5 | 0.7 |
| 1849 | 1.8 | 0.8 | 0.90 | 24.0 | 0.96 | 28.0 | 3.9 | 1.5 | 4.0 |
| 1957 | 1.5 | 0.7 | 4.00 | 24.6 | 0.99 | 33.2 | 16.0 | 1.0 | 8.6 |
| 199-201 | 5.0 | 2.7 | 11.00 | 28.4 | 2.89 | 30.0 | 25.0 | 200.0 | 1.6 |
| 2057 | 9.5 | 4.5 | 4.00 | 25.0 | 5.27 | 29.0 | 17.0 | 1.5 | 4.0 |
| 211 | 12.0 | 6.2 | 2.50 | 27.3 | 7.00 | 30.3 | 10.5 | 95.0 | 3.0 |
| 213 | 21.5 | 9.0 | 1.00 | 22.7 | 10.70 | 26.5 | 2.7 | 0.7 | 3.8 |
| 2131 | 1.9 | 0.8 | 0.25 | 22.8 | 0.97 | 26.8 | 0.3 | 0.3 | 4.0 |
| 214 | 18.0 | 8.0 | 2.50 | 24.0 | 10.00 | 29.0 | 9.1 | 1.1 | 5.0 |
| 215 | 22.0 | 12.3 | 15.30 | 29.2 | 13.00 | 30.6 | 17.0 | 3.3 | 1.4 |
| 217 | 14.0 | 7.3 | 3.50 | 27.5 | 8.80 | 32.0 | 21.3 | 360.0 | 4.5 |

TABLE 5.3a Friction on worn granite surfaces
Experiment 1957 N = 1.5 MPa

| Experiment | Shear Load MPa | Displacement mm | | ϕ | Time min |
|--------------------|-------------------|-----------------|--------|--------|-------------|
| | | From | To | | |
| Load to first slip | 0.686 | 0.00 | 4.063 | 24.6 | 12.52 |
| Creep run 0 | 0.700 | 4.063 | 5.133 | | |
| Load to creep 1 | 0.7122 | 5.133 | 11.055 | 25.4 | 44.85 |
| Creep run 1 | 0.820 | 11.055 | 11.495 | | |
| Load to creep 2 | 0.917 | 11.495 | 12.613 | 31.4 | 45.15 |
| Creep run 2 | 0.954 | 12.613 | 12.686 | | |
| Load to creep 3 | 0.960 | 12.686 | 14.020 | 32.62 | 55.87 |
| Creep run 3 | 0.975 | 14.020 | 14.113 | | |
| Load to creep 4 | 0.983 | 14.113 | 16.052 | 33.2 | 65.17 |
| Creep run 4 | 0.991 | 16.052 | 16.114 | | |

TABLE 5.3b Friction on worn granite surfaces
Experiment 127 N = 9.0 MPa

| Experiment | Shear Load MPa | Displacement mm | | ϕ° | Time hrs |
|--------------------|-------------------|-----------------|--------|--------------|-------------|
| | | From | To | | |
| Load to first slip | 3.912 | 0.00 | 0.193 | 23.5 | 168 |
| Creep run 0 | 4.037 | 0.193 | .534 | | |
| Load to creep 1 | 4.213 | 0.534 | 0.962 | 25.1 | 216 |
| Creep run 1 | 4.252 | 0.962 | 0.993 | | |
| Load to creep 2 | 4.483 | 0.993 | 3.519 | 26.5 | 240 |
| Creep run 2 | 4.534 | 3.519 | 5.349 | | |
| Load to creep 3 | 4.626 | 5.349 | 8.099 | 27.2 | 288 |
| Creep run 3 | 4.583 | 8.099 | 8.099 | | |
| Load to creep 4 | 4.751 | 8.099 | 8.104 | 28.0 | 336 |
| Creep run 4 | 5.005 | 8.104 | 12.688 | | |

TABLE 5.3c Friction on worn granite surfaces
Experiment 217 N = 14.0 MPa

| Experiment | Shear Load MPa | Displacement mm | | ϕ° | Time hrs |
|--------------------|-------------------|-----------------|--------|--------------|-------------|
| | | From | To | | |
| Load to first slip | 7.297 | 0.00 | 3.497 | 27.5 | 0-52 |
| Creep run 0 | 7.296 | 3.497 | 3.525 | | 53-118 |
| Load to creep 1 | 7.348 | 3.535 | 5.137 | 27.7 | 199-166 |
| Creep run 1 | 7.350 | 5.137 | 5.163 | | |
| Load to creep 2 | 7.480 | 5.163 | 5.524 | 28.1 | 167-172 |
| Creep run 2 | 7.481 | 5.524 | 7.514 | | |
| Load to creep 3 | 7.559 | 7.514 | 8.075 | 28.4 | 123-211 |
| Creep run 3 | 7.558 | 8.075 | 8.275 | | |
| Load to creep 4 | 7.723 | 8.275 | 9.335 | 28.9 | 212-236 |
| Creep run 4 | 7.722 | 9.335 | 9.529 | | |
| Load to creep 5 | 7.883 | 9.529 | 14.457 | 29.4 | 237-263 |
| Creep run 5 | 7.882 | 14.457 | 15.275 | | |
| Load to creep 6 | 8.065 | 15.275 | 15.286 | 29.9 | 264-283 |
| Creep run 6 | 8.064 | 15.286 | 15.291 | | |
| Load to creep 7 | 8.104 | 15.291 | 17.174 | 30.1 | 284-308 |
| Creep run 7 | 8.105 | 17.174 | 17.595 | | |
| Load to creep 8 | 8.175 | 17.595 | 18.574 | 30.3 | 309-332 |
| Creep run 8 | 8.176 | 18.574 | 18.737 | | |
| Load to creep 9 | 8.255 | 18.737 | 19.566 | 30.5 | 333-337 |
| Creep run 9 | 8.255 | 19.566 | 20.010 | | |
| Load to creep 10 | 8.413 | 20.010 | 20.424 | 31.0 | 338-360 |
| Creep run 10 | 8.414 | 20.424 | 21.305 | | |
| Final run | 8.793 | 21.305 | 21.314 | 32.13 | 360-360.164 |

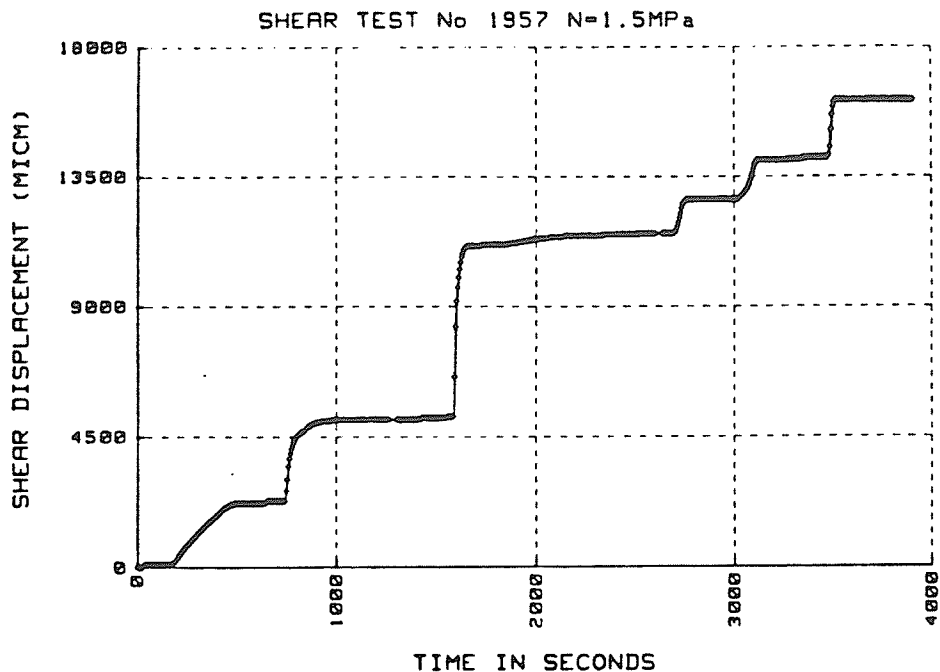


Fig. 5.3a The variation of the displacement with time in an incremented-load test. Loads are listed in Table 5.3a. The normal load was relatively low

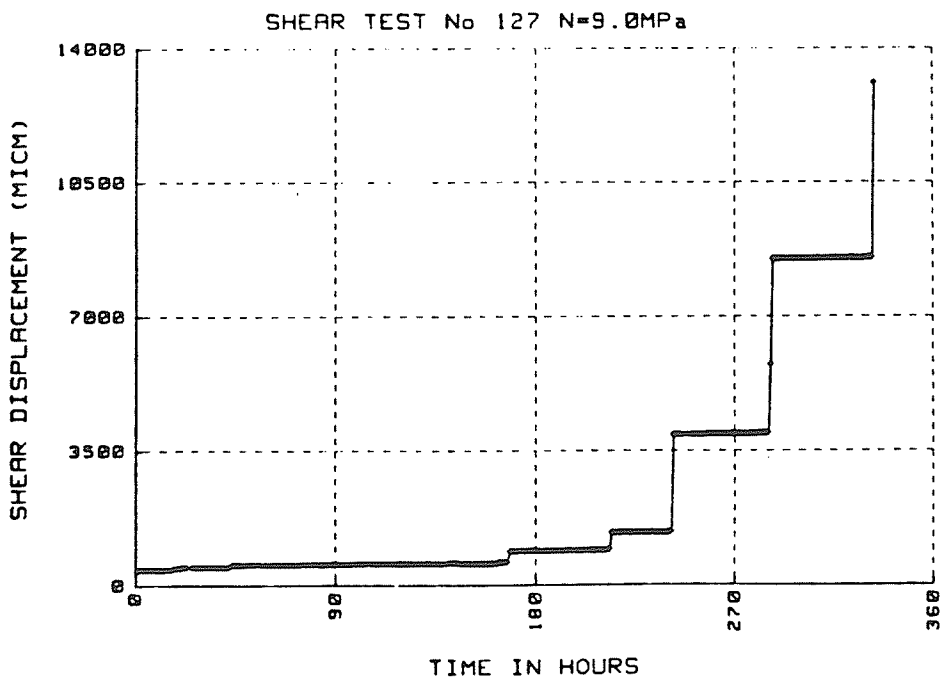


Fig. 5.3b The variation of the displacement with time in an incremented-load test. Loads are listed in Table 5.3b. The normal load was "intermediate"

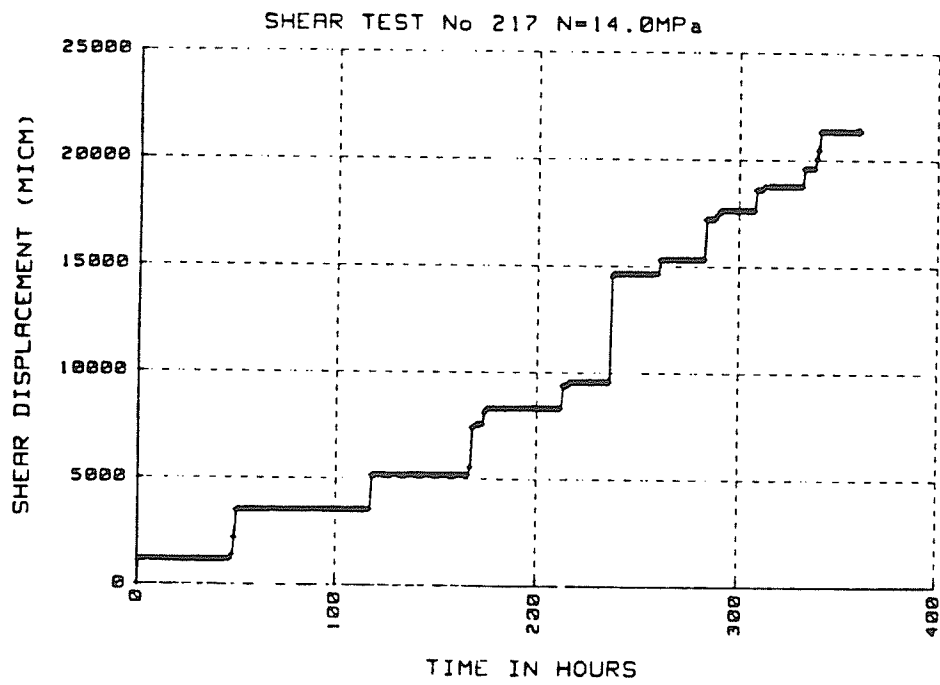


Fig. 5.3c The variation of the displacement with time in an incremented-load test. Loads are listed in Table 5.3c. The normal load was "high"

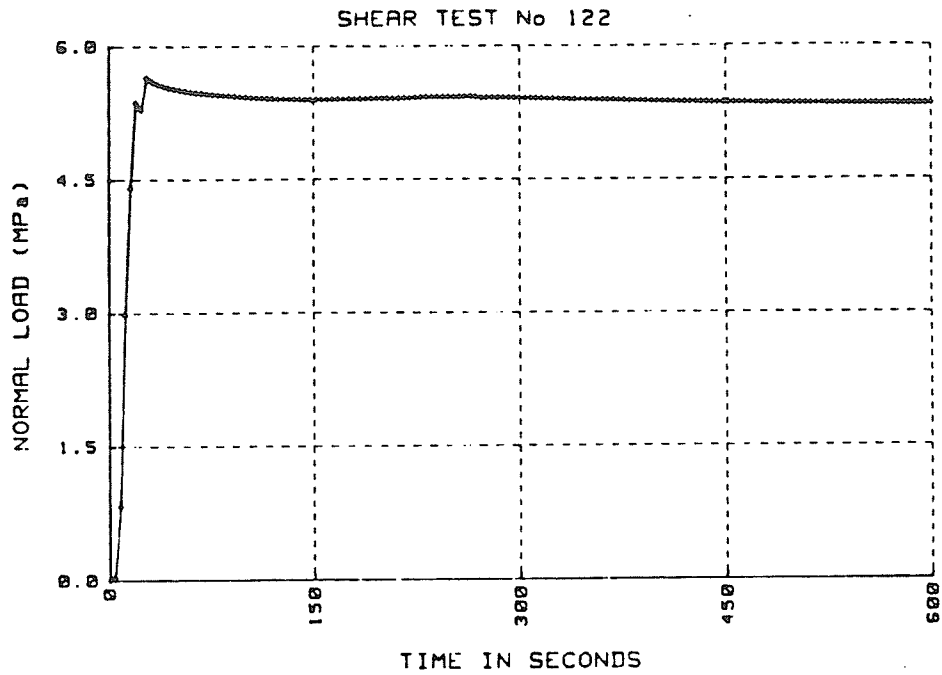


Fig. 5.4 The normal load in test 122

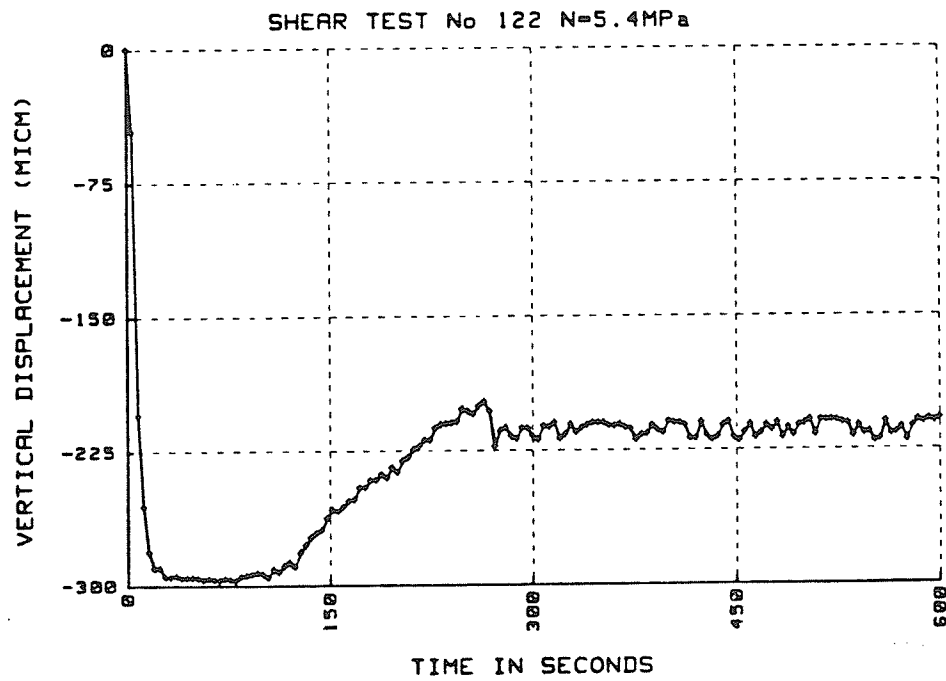


Fig. 5.5 The vertical displacement versus time curve in test 122

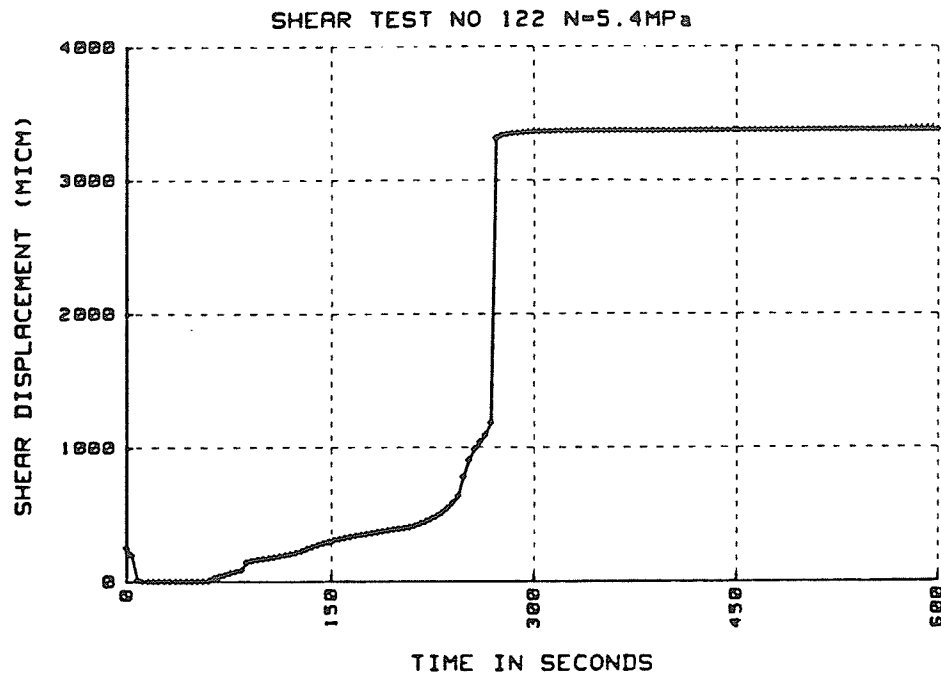


Fig. 5.6 The horizontal displacement versus time curve for test

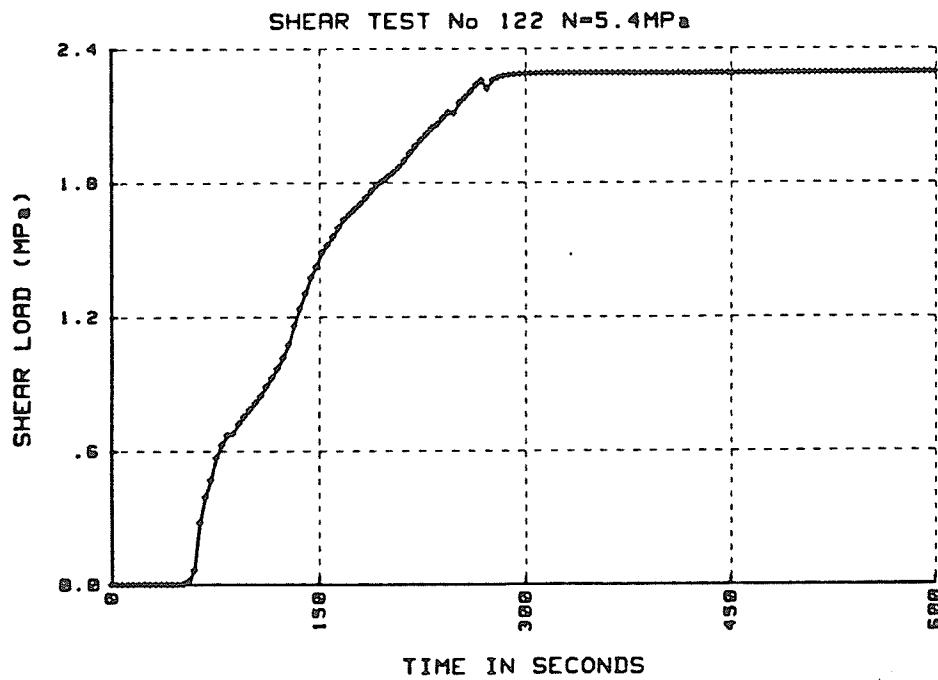


Fig. 5.7 The shear load in test 122

dilation in the normal direction (Fig. 5.5) and limited movement in the shear direction (Fig. 5.6).

3. At the moment of first slip, two events were observed: sudden horizontal movement (Fig. 5.6) and vertical closure (Fig. 5.5).

This behaviour was observed in all tests, regardless of the magnitude of the normal load. There is, however, a difference in the shape of the displacement curves after the first slip had occurred, depending mainly on the magnitude of the normal load and presence or absence of stick-slip events. After first slip, one of two processes may occur. In some cases horizontal or shear displacement decelerates in a stable manner, i.e. without stick-slip events (Fig. 5.8). In most cases, however, movement would continue while accompanied by stick-slip events. Whether one or the other occurs depends on the shear load. In the hydraulically controlled direct shear test, the shear load tends to fall after each stick-slip event, then increases again. If, for some reason, the shear load does not reach the previous peak load, then the movement decelerates slowly without further stick-slip events (stable sliding). The displacement versus time curve in this case assumes a shape that is typical of a transient creep curve (Fig. 5.8). When however the shear load increases above the previous peak, shear displacement, accompanied by stick-slip events, continues on (Fig. 5.9). The stick-slip events would register on the displacement curves somewhat differently for low and high normal load. The shear displacement versus time curve would show steps in both cases. At low normal load these steps would have steep risers and flat steps (Fig. 5.10). At high normal load (Fig. 5.11) the edges

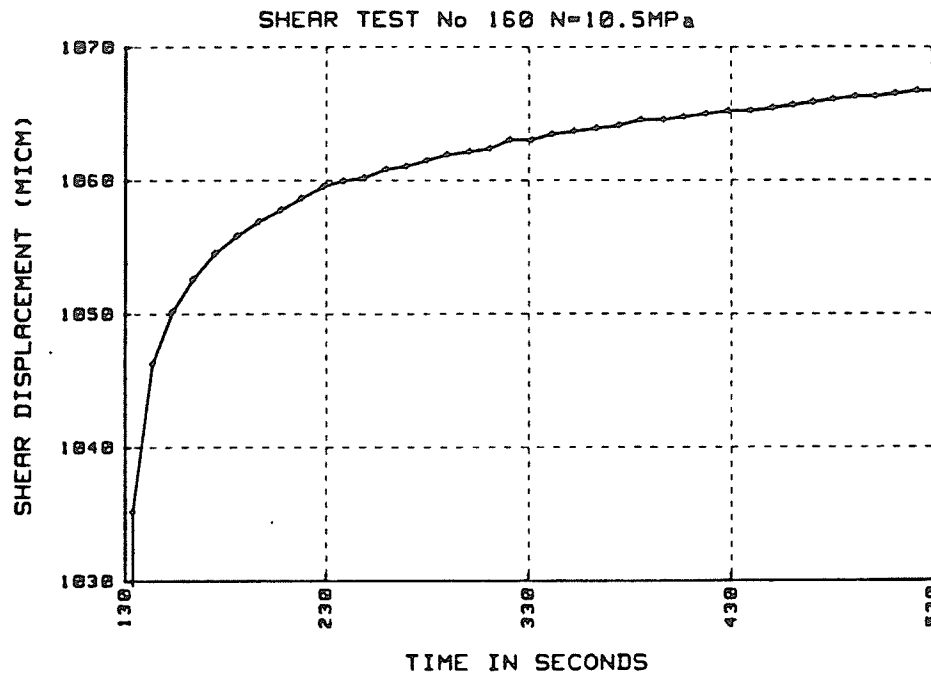


Fig. 5.8 An example of stable sliding

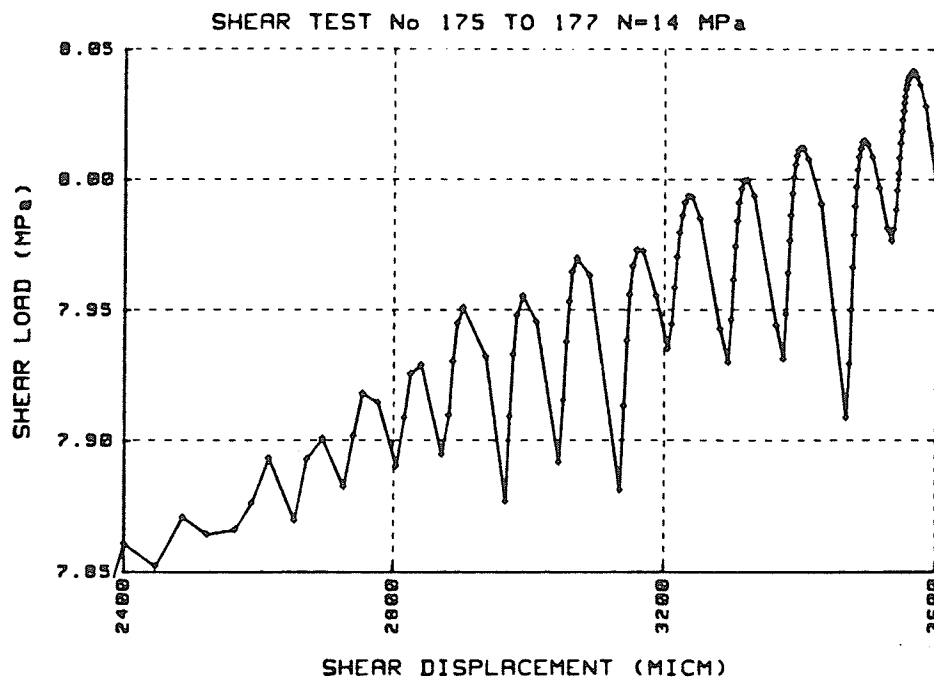


Fig. 5.9 Stick-slip events

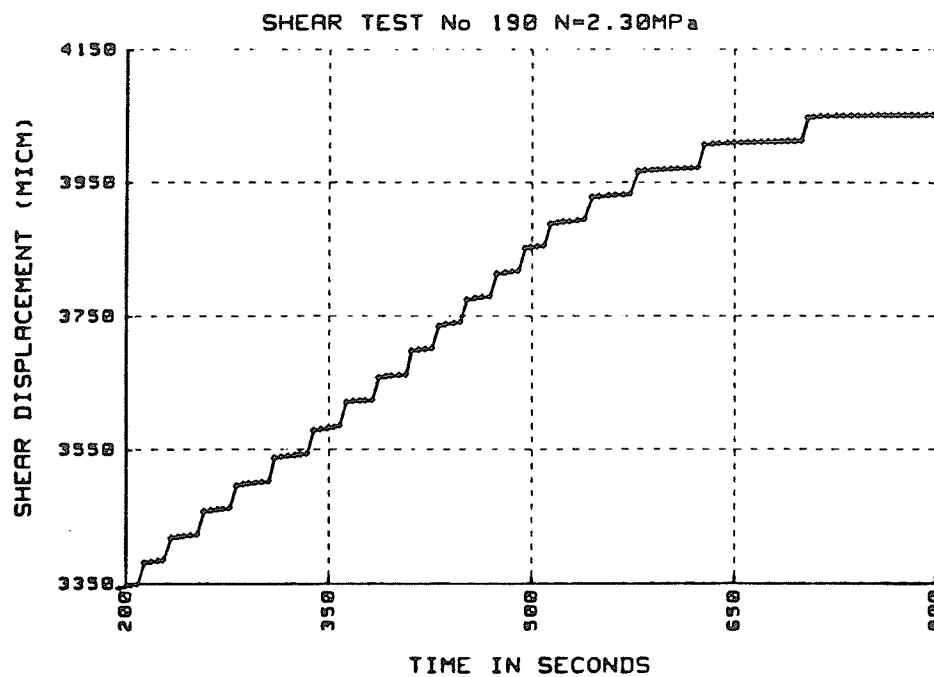


Fig. 5.10 Shear displacement versus time at low normal load

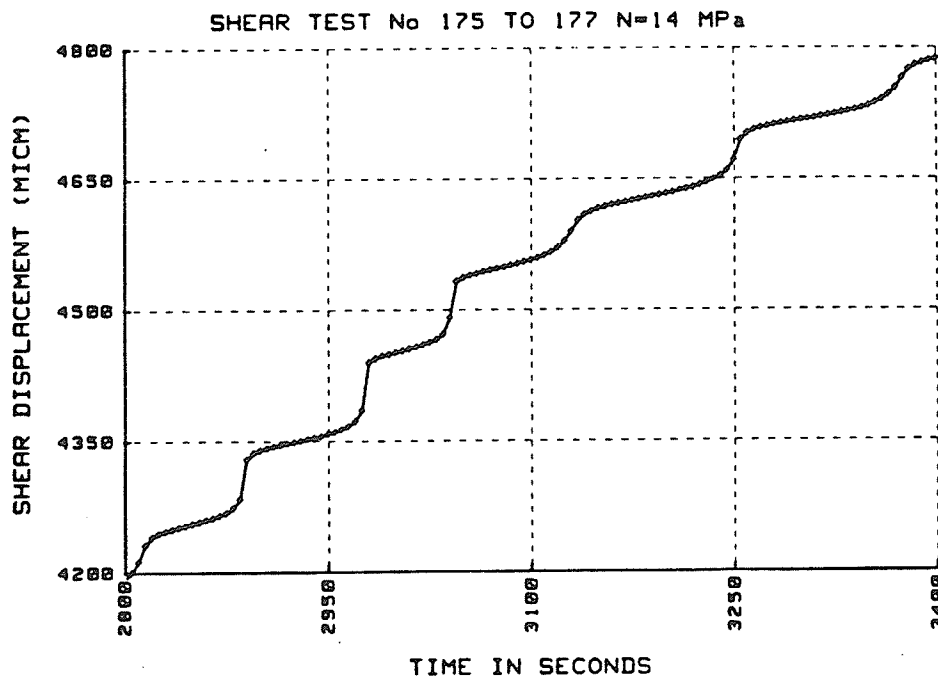


Fig. 5.11 Shear displacement versus time at high normal load

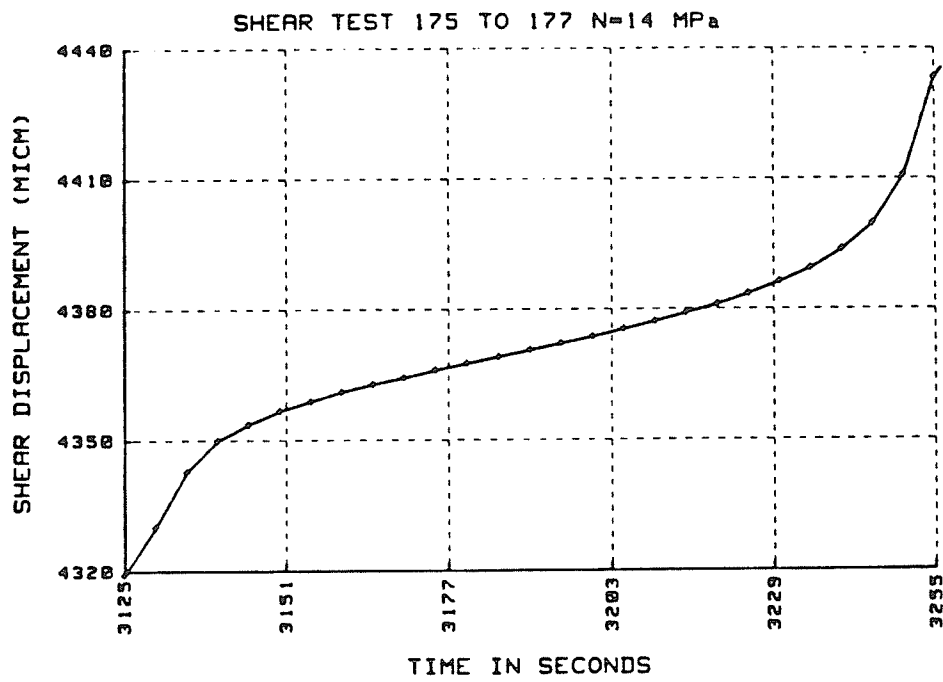


Fig. 5.12 The fifth "step" of Figure 5.11 shown in detail

appear "rounded off" and each step would assume a shape suggesting a full transient to tertiary creep curve (Fig. 5.12). During stick slip events, the normal displacement curve indicates progressive closure. Here again closure tends to be more gradual when the normal load is high (Fig. 5.13) and rather abrupt when the normal load is small (Fig. 5.14).

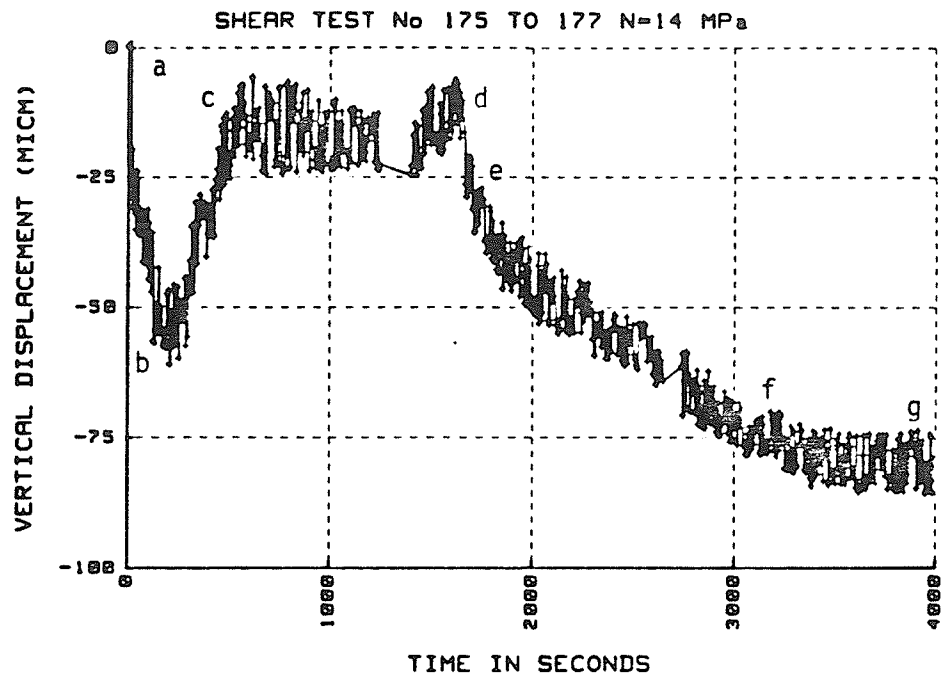


Fig. 5.13 Vertical displacement versus time at high normal load, starting with normal load application (a-b), shear load application (b-c) at constant shear load (c-d), closure on incremented load (d-c) and gradual closure during stick slip (e-f) displacement stops (f-g)

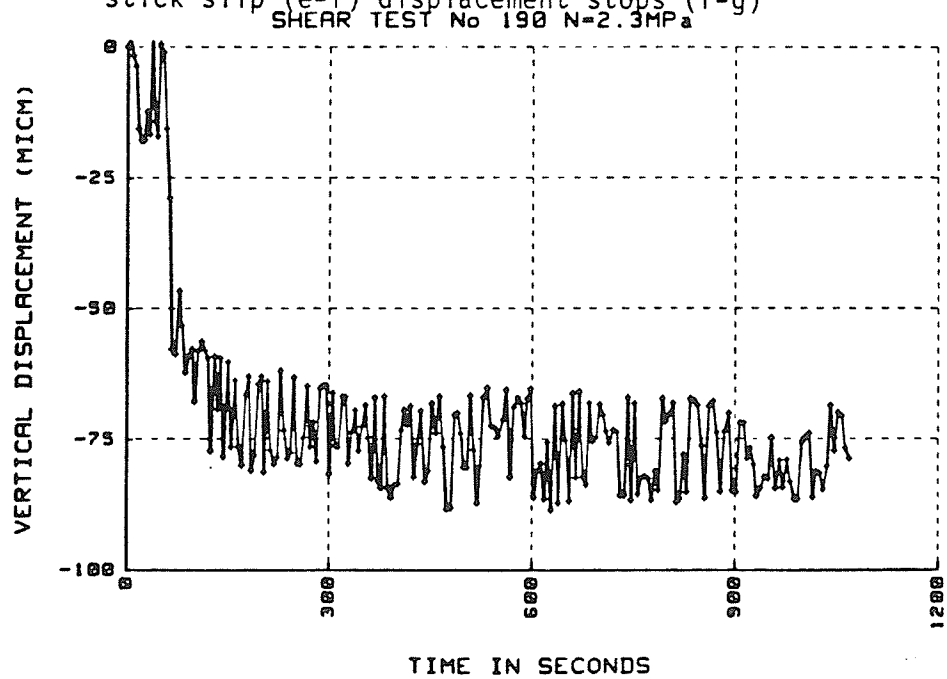


Fig. 5.14 The same as in Figure 5.13 but at low normal load

CHAPTER 6

DISCUSSION, SUMMARY AND CONCLUSION

6.1 SUMMARY OF RESULTS

The results of this testing program may be summarized as follows:

1. In all tests, shear deformation progressed in a "stick-slip" manner as between points a and b of Fig. 6.1 and (Fig. 6.2a,b). However, not all the shear load versus shear displacement curves register "stick-slip events". Their detection requires either continuous measurement (e.g. using a plotter) or frequent recording of the digital output. The HP system that was used for most of the experiments needed about 4 seconds to recycle and no doubt some of the stick-slip cycles could have been missed. When measurement cycles were set at lower intervals, stick-slip movement could easily be missed.
2. In order to have continuous shear displacement, the shear load needs to be raised continuously (Fig. 6.3). At constant shear load (Fig. 6.3) displacement soon comes to a halt (Fig. 6.1). In all cases, where large shear displacement was achieved, the shear load was increased several times.
3. The stick-slip movement is accompanied by cycling of the shear load between limits. The amplitude of these vibrations however was not constant: and it is possibly influenced by the reaction time of the hydraulic loading system. In addition, the data acquisition system may have missed the tops and bottoms.
4. In general, after each stick-slip event, the vertical displacement

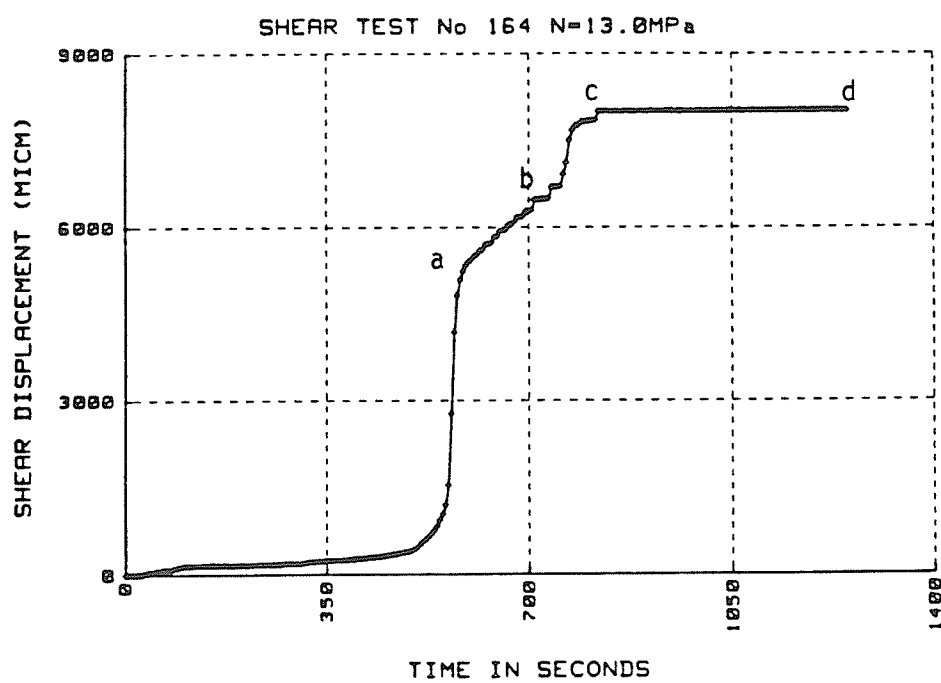


Fig. 6.1 Displacement during stick slip (a-b); displacement ceased while shear load constant (c-d)

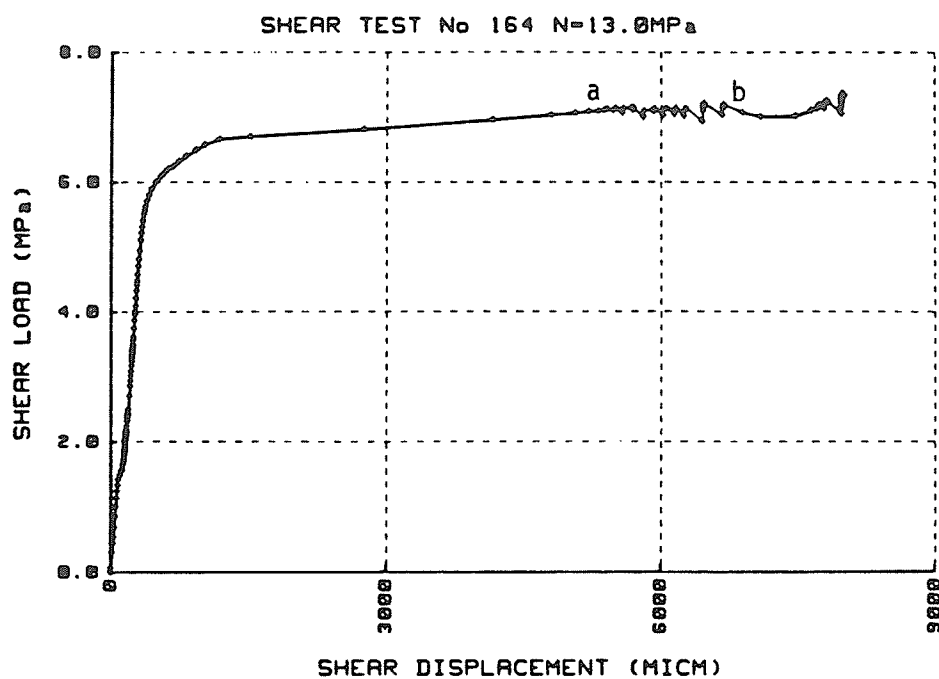


Fig. 6.2a The load displacement curve showing the shear load increasing between a and b of Figure 6.1

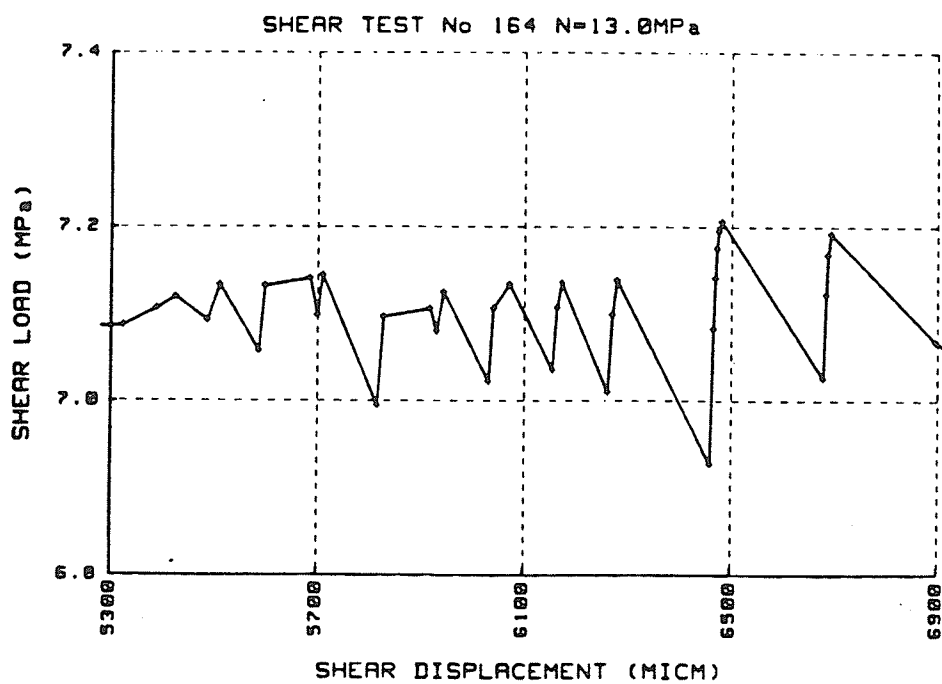


Fig. 6.2b Stick-slip events of Figure 6.2a in detail

(Fig. 6.4) would indicate progressive closure between the two rock blocks. This is more obvious at high rather than at low normal load (Fig. 5.13) and (Fig. 5.14).

5. The shear displacement versus time curve is never smooth. It may appear so when the curve is displayed to show the "total" displacement curve (Fig. 6.5a,b,c). At a finer scale (Fig. 6.5d) the curve shows distinct steps. The steps themselves appear to consist of straight risers and flat steps when the normal load is small, about 2.30 MPa (Fig. 5.9) or quite curved when the normal load is large, about 14.0 MPa (Fig. 5.11). Indeed in the latter case the steps appear to be "creep curves" where the risers mark the position of "tertiary" and the flats the transient and perhaps steady parts of a creep curve (Fig. 5.12).
6. Once stick-slip movement comes to a halt, the displacement curve becomes "smoother" as the stick-slip related steps gradually die out (Fig. 6.6) and (Fig. 6.7) and movement soon stops.
7. Once displacement ceased, only an increase in the shear load could start the movement again. There seemed to be no end of this process and it appears that the long-term strength could increase further (Fig. 5.2c), (Fig. 6.8) and (Fig. 6.9). In this program, it was limited by the allowable movement of the testing machine (about 2.5 cm).

6.2 INTERPRETATION OF RESULTS IN TERMS OF THE ADHESION THEORY

It appears that all the experimental results from friction tests using a worn granite surface can be interpreted with the help

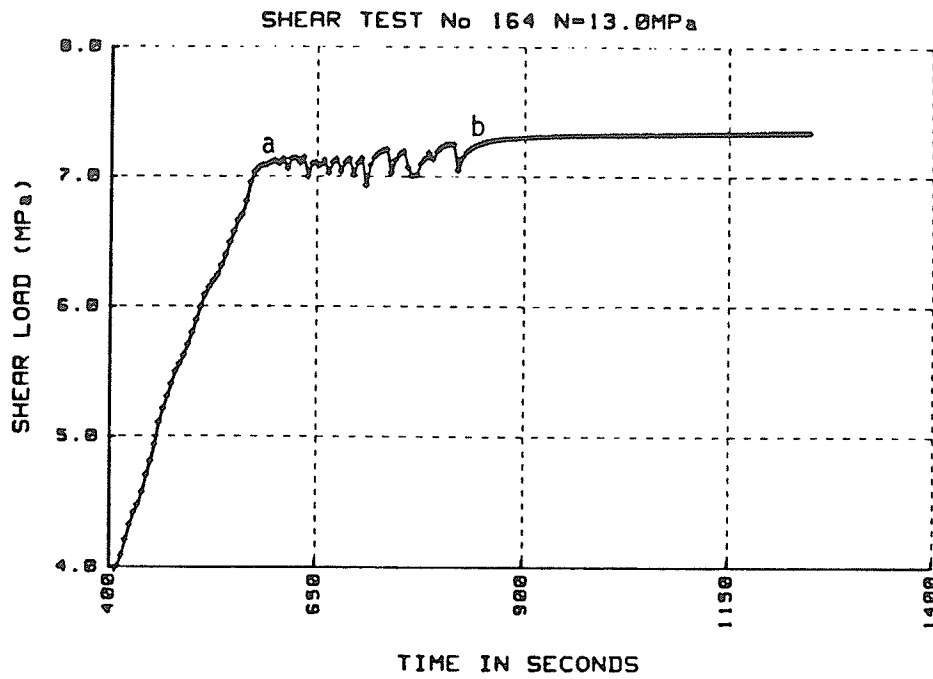


Fig. 6.3 The shear load versus time for the test of Figures 6.1 to 6.2

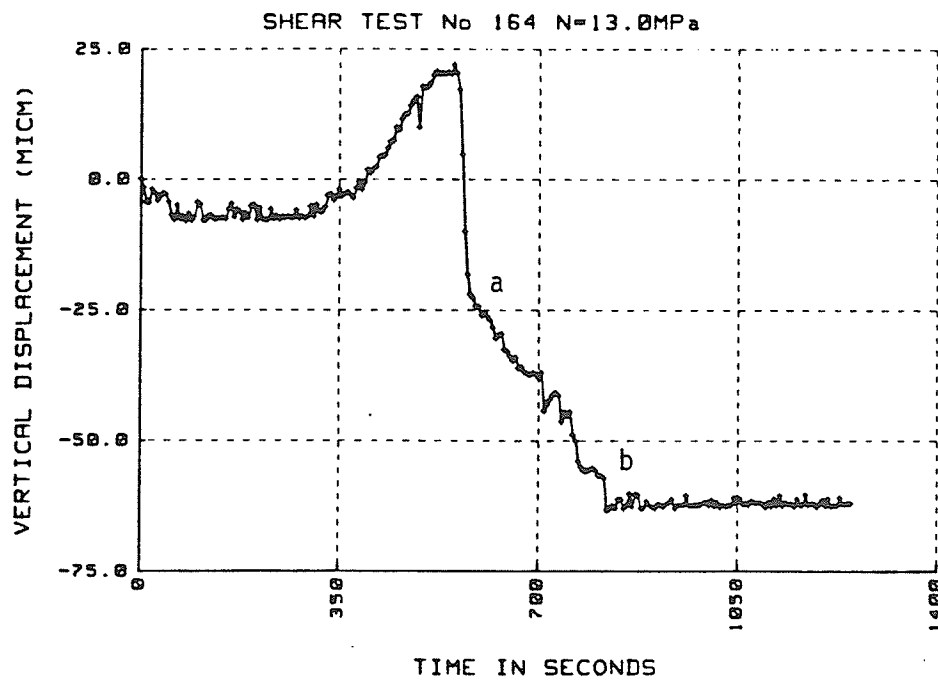


Fig. 6.4 Vertical displacement versus time, point a to b show closure during stick slip

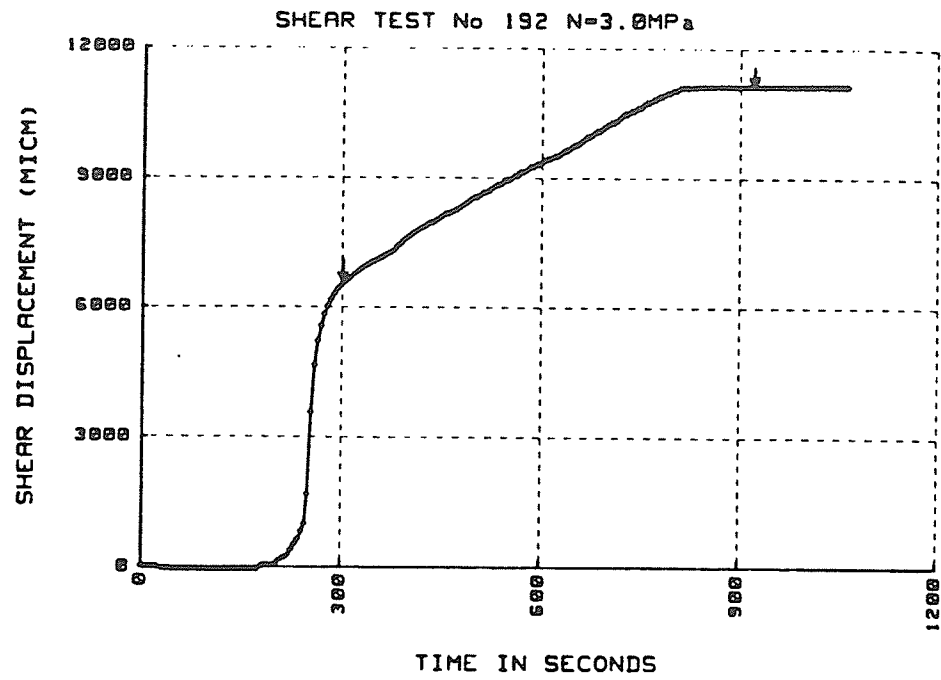


Fig. 6.5a Shear displacement versus time in a low-normal load test. Although the curve between the arrows appears to be relatively smooth, subsequent figures will show that it is not

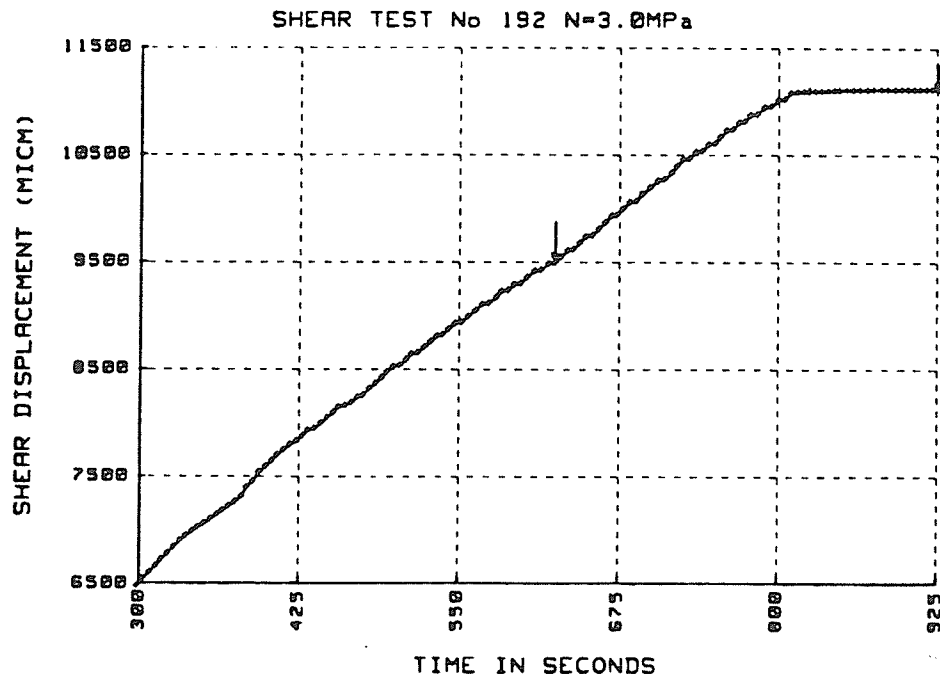


Fig. 6.5b Shear displacement versus time

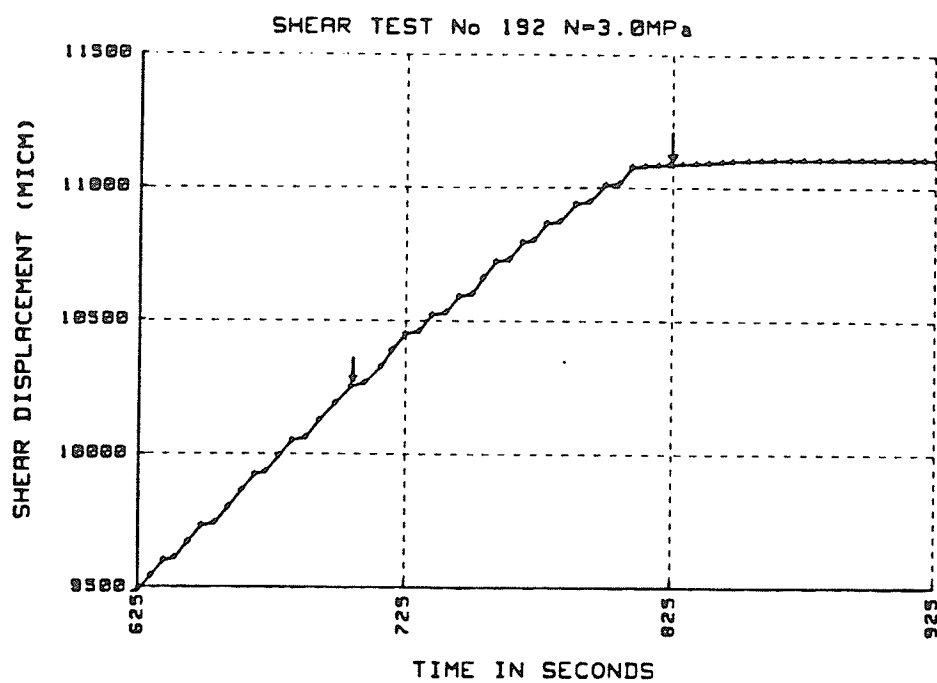


Fig. 6.5c Shear displacement versus time

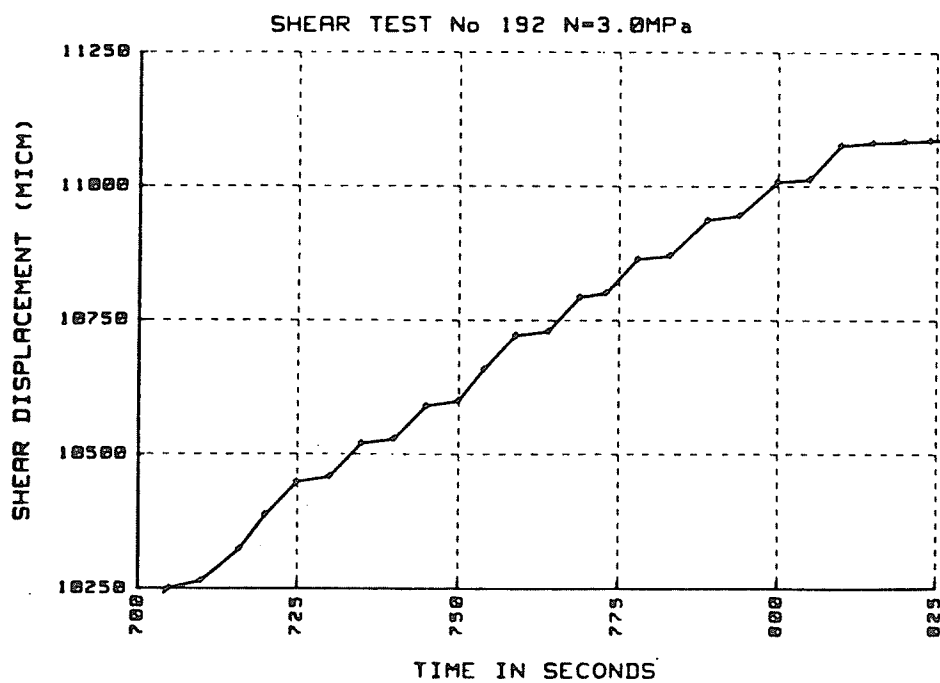


Fig. 6.5d Shear displacement versus time

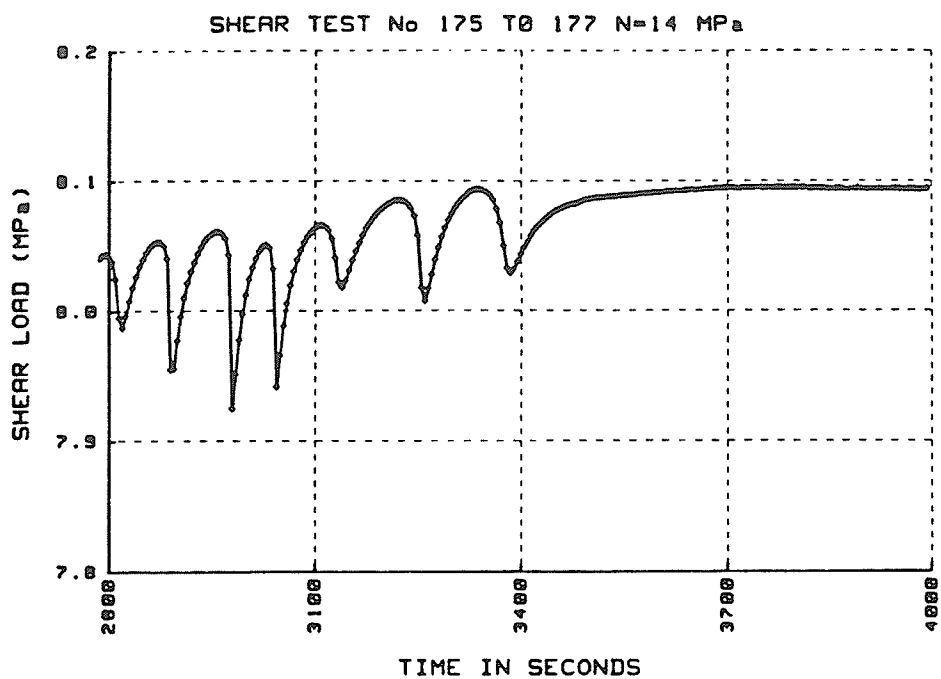


Fig. 6.6 Shear load versus time. The end of stick-slip

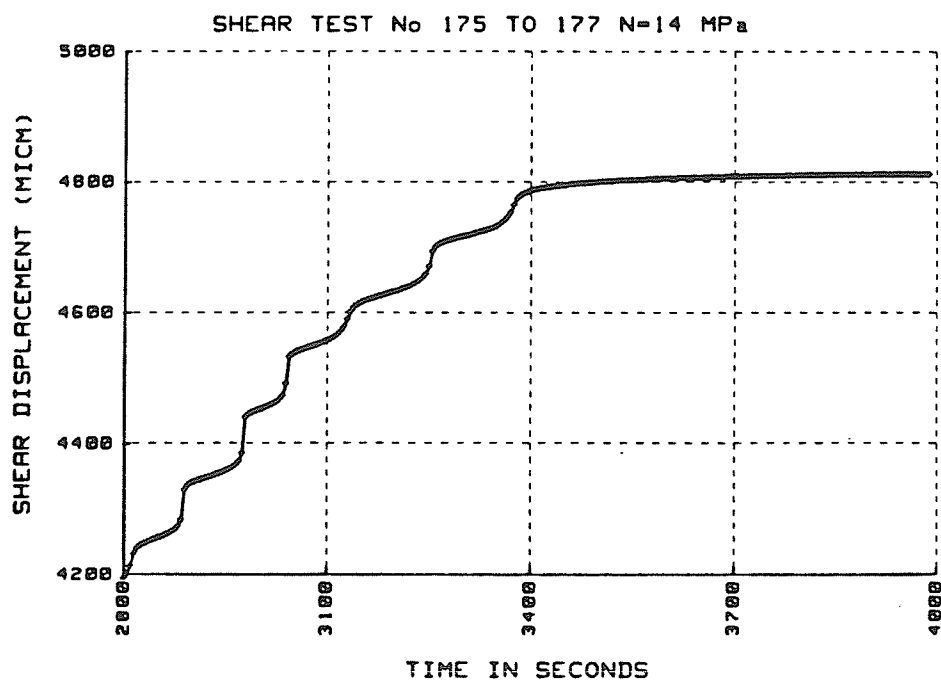


Fig. 6.7 Shear displacement versus time. The end of stick-slip

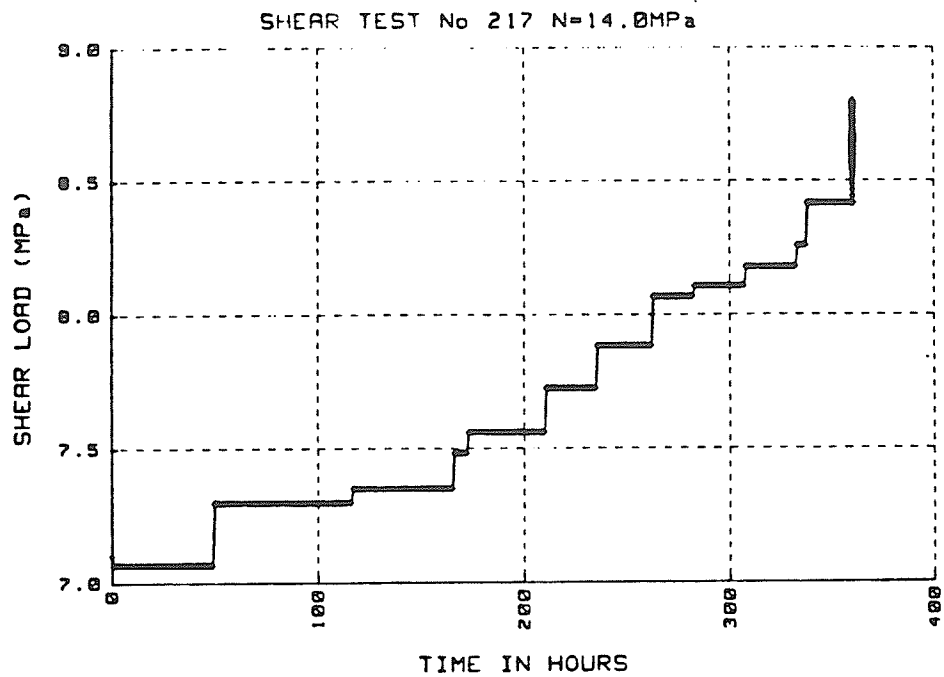


Fig. 6.8 The load history of test 217. The first slip occurred at about hour 50. Details found in Table 5.3c. Each step in load caused a slip

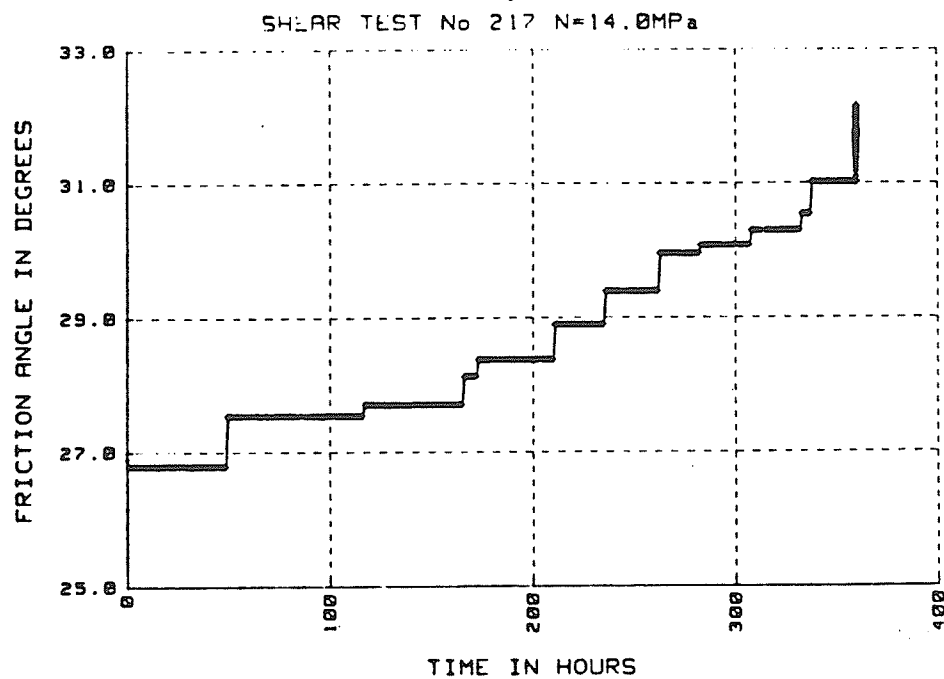


Fig. 6.9 The increase in frictional resistance with time during test 217

of the adhesion theory.

The experimental series in which frictional resistance was measured as a function of the duration of stick at constant normal load demonstrates the increase in frictional resistance through creep deformation of asperities alone, since no shear load was applied to cause shear displacement (Fig. 5.1a). When there is a shear load high enough to cause shear displacement (as opposed to shear deformation), asperities are fractured. When this happens, closure is seen to occur (Fig. 5.13), and consequently the true area of contact must increase. Movement comes to a halt and the shear load must be increased for further displacement. Accordingly, there appear to be two ways to increase the long-term frictional resistance. First, the true contact area may increase through the transient or steady state creep of the asperities. Second, on increasing shear the asperities may fracture, allowing shear displacement to occur. This is followed by closure causing the contact area to increase.

In a shear test both processes take place concurrently though there is an indication that the first process is not as important when the normal load is low (Fig. 5.14).

Clearly, one must then accept the consequence of the adhesion theory that there is no upper limit to frictional resistance, provided that both mechanisms are fully utilized. Essentially this translates into the requirement that the load should not be allowed to increase at a higher rate than the available frictional resistance. Conceptually, with an ever-increasing true contact area, the discontinuity should disappear with time as the molecules on two sides of discontinuity come closer to each other, the adhesive forces between

them should increase to approaching a magnitude that exists between molecules of the intact rock itself.

It must be clearly stated that the results of this investigation apply only to a flat and macroscopically smooth surface that has undergone previous shear deformation. Macroscopically rough surfaces like those discussed by Barton (1971), present a different problem that is not within the scope of this investigation.

The results however have a number of implications with respect to the long-term strength of the rock mass. Most importantly, it identifies the "intact rock" component of the rock mass as the one being mainly responsible for the usually experienced time dependent weakening of the rock mass. Furthermore, intact rock is identified as a very important participant in frictional resistance through the creep and fracture of the microscopic asperities that themselves are composed of intact rock.

Future investigations should incorporate rough surfaces, like those occurring on rock joints (extension fractures) and surfaces that are coated with alteration products. Similar investigations with other rock types, perhaps less brittle than granite are also recommended. An additional contribution could come from improved loading systems. In particular, the tilting cable-assembly for the normal load could be replaced with a construction that allows the normal load to travel with the specimen. The shear loading, in turn, would benefit from a "closed-loop" type of electronic control that would provide for both constant load or constant rate loading.

REFERENCES

- Amadei, B. and Curran, J.H. (1980). "Creep behaviour of rock joints". Proc. 13th Can. Rock Mech. Symp., pp. 146-150.
- Barton, N.R. (1971). "A relationship between joint roughness and joint shear strength". Rock Fracture, Proc. of Int. Symp. on Rock Mech. Nancy, France.
- Barton, N.R. (1974). "Estimating the shear strength of rock joints". Proc. 3rd Congress I.S.R.M. Denver, pp. 219-220.
- Bowden, F.P. (1954). "The friction of non-metallic solids". J. Inst. Petrol., 40, pp. 89-103.
- Bowden, F.P. and Leben. (1939). "The nature of sliding and the analysis of friction". Proc. Roy. Soc., London, A169-371-391.
- Bowden, F.P., Moore, A.J. and Tabor, D. (1943). "The ploughing and adhesion of sliding metals". J. App. Phy., 14, pp. 80-91.
- Bowden, F.P. and Tabor, D. (1964). "The friction and lubrication of solids". Vol. 2, Clarendon, London Publ.
- Bowden, F.P. and Tabor, D. (1973). "Friction". Doubleday & Company, Inc. New York.
- Brace, W.F. and Byerlee, J.D. (1966). "Recent experimental studies of brittle fracture of rocks". Proc. 8th Symposium on Rock Mechanics, pp. 58-81.
- Bruce, I. (1978). Ph.D. Thesis, University of Alberta, Edmonton, Alberta.
- Byerlee, J.D. (1967a). "Theory of friction based on brittle fracture". J. of Appl. Physics, 38, pp. 2928-2934.
- Byerlee, J.D. (1967b). "Frictional characteristics of granite under high confining pressure". J. of Geophysical Research, Vol. 72, No. 14, pp. 3539-3647.
- Byerlee, J.D. (1970). "The mechanics of stick-slip". Tectonophysics, 9, pp. 475-486.
- Byerlee, J.D. (1978). "Friction of rocks". Pageophy., Vol. 116, pp. 615-625.
- Byerlee, J.D. and Brace, W.F. (1968). "Stick-slip, stable sliding and earthquakes. Effect on rock type, pressure, strain rate and stiffness". J. of Geophysical Research, Vol. 73, No. 18, pp. 6031-6037.

- Coulomb, C.A. (1781). "Theory of simple machines". Paris, Bachelier, Libraire, Quai des Augustins. 1821.
- Coulson, J.H. (1970). "The effects of surface roughness on the shear strength of joints in rock". Technical Report MRD 2-70, Missouri River Division, Corps of Engineers, Omaha.
- Coulson, J.H. (1972). "Shear strength of flat surfaces in rock". ASCE, 13th Symp. on Rock Mech., pp. 77-105.
- Dieterich, J.H. (1972). "Time-dependent friction in rocks". J. Geophys. Res. 77, pp. 3771-3781.
- Dieterich, J.H. (1978). "Time-dependent friction and the mechanism of stick-slip". Pageophy., 116, pp. 790-805.
- Engelder, J.T. (1974). "Microscopic wear grooves on slickensides: indicators of paleoseismicity". J. Geoph. Res. 79, pp. 4387-4392.
- Engelder, J.T. (1978). "Aspect of asperity surface interaction and surface damage of rocks during experimental friction sliding". Pageophy., Vol. 116, pp. 705-716.
- Engelder, J.T. and Scholz, C.H. (1976). "The role of asperity indentation and ploughing in rock friction, influence of relative hardness and normal load". Int. J. Rock Mech. and Min. Sci., Vol. 13, pp. 155-163.
- Horn, H.M. and Deere, D.N. (1962). "Frictional characteristics of minerals". Geotechnique, 12, 319-335.
- Hoskins, E.R., Jaeger, J.C. and Rosengren, K.J. (1968). "A medium scale direct friction experiment". Int. J. Rock Mech. Min. Sci., 5, pp. 143-154.
- Jaeger, J.C. (1959). "The frictional properties of joints in rocks". Geofis. Pura. App., 43, pp. 148-158.
- Jaeger, J.C. and Cook, N.G.W. (1979). "Fundamentals of Rock Mech. Fletcher and Son Ltd., Norwich, London.
- Lajtai, E.Z. (1981). "Creep and crack growth in Lac du Bonnet granite due to compressive strength". Proc. of 5th Can. Fracture Mech. Conf., Winnipeg, Manitoba.
- Lajtai, E.Z. (1985). "The time-dependency of rock strength". CIM 9th District Four Meeting, Thompson, Manitoba.
- Krahn, J. (1979). "The ultimate frictional resistance of rock discontinuities". Int. J. Rock Mech. Min. Sci. and Geomech. Abstr., Vol. 16, pp. 127-133.
- Miller, D.R. (1962). "Friction and abrasion of hard solids at high

sliding speed". Proc. Royal Society of London, Vol. A269, pp. 368-384.

Moore, D.F. (1975). "Principles and applications of tribology". Wheaton & Co., Exeter, Great Britain.

Newland, P.L. and Allely, B.H. (1957). "Volume changes in drained triaxial tests on granular material". Geotech. Vol. 7, No. 1, pp. 17-34.

Patton, D. (1966). "Multiple modes of shear failure in rock". Proc. 1st Congress I.S.R.M., Lisbon, V. 1, pp. 409-513.

Penman, A.D.M. (1953). "Shear characteristics of a saturated silt measured in triaxial compression". Geotechnique, 3, pp. 312-328.

Rabinowicz, E. (1965). "Friction and wear of materials". John Wiley and Son. Publ.

Scholz, C.H. (1972). "Static fatigue of quartz". J. Geoph. Res., 77, p. 2104.

Scholz, C.H. and Engelder, J.T. (1976). "The role of asperity indentation and ploughing in rock friction, asperity creep and stick-slip". Int. J. Rock Mech. and Min. Sci., Vol. 13, pp. 149-154.

Terzaghi, K. Van and Peck, R.B. (1948). "Soil mechanics in engineering practice". New York, John Wiley & Sons, Inc.

Teufel, L.W. and Logan, J.M. (1978). "Effect of displacement rate on the real area of contact and temperatures generated during frictional sliding of Tennessee sandstone". Pure and Appl. Geophys., Vol. 116, pp. 840-865.